Microelectrode cluster technology for precise interactions with neuronal circuits. Towards highly specific adaptive deep brain stimulation.

Mohammed, Mohsin

2020

Document Version:
Publisher's PDF, also known as Version of record

Microelectrode cluster technology for precise interactions with neuronal circuits

Towards highly specific adaptive deep brain stimulation

MOHSIN MOHAMMED
EXPERIMENTAL MEDICAL SCIENCE | FACULTY OF MEDICINE | LUND UNIVERSITY

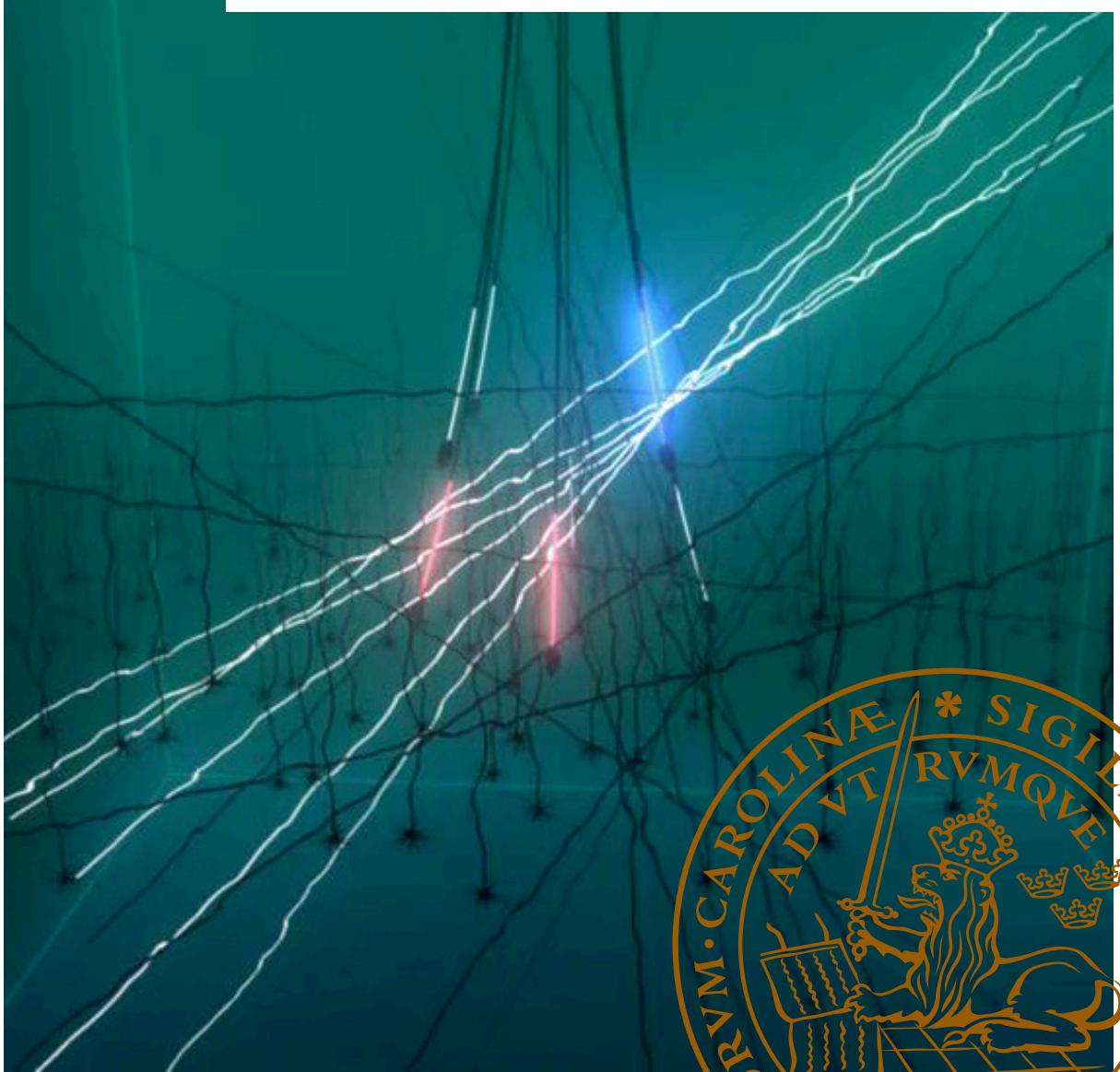

Printed by Media-Tryck, Lund 2020 NORDIC SWAN ECOLABEL 3041 0903

LUND UNIVERSITY

FACULTY OF MEDICINE

Department of
Experimental Medical Science

Lund University, Faculty of Medicine
Doctoral Dissertation Series 2020:126
ISBN 978-91-7619-989-3
ISSN 1652-8220

Microelectrode cluster technology for precise interactions with neuronal circuits

Microelectrode cluster technology for precise interactions with neuronal circuits

Towards highly specific adaptive deep brain stimulation

Mohsin Mohammed

LUND
UNIVERSITY

DOCTORAL DISSERTATION
by due permission of the Faculty of Medicine, Lund University, Sweden.
To be defended at Hörsalen, Medicon Village, Lund, on Monday, the 30th of November 2020 at 9.00 am.

Faculty opponent
Professor Johan Wessberg, Department of Physiology, Institute of Neuroscience and Physiology, Gothenburg University.

Organization LUND UNIVERSITY Department of experimental Medical Science, Faculty of Medicine Author: Mohsin Mohammed	**Document name** DOCTORAL DISSERTATION **Date of issue** 2020-11-30 **Sponsoring organization**: Swedish Research Council, Knut and Alice Wallenberg Foundation, Lund University, Region Skåne, Neuronano AB.

Title and subtitle: Microelectrode cluster technology for precise interactions with neuronal circuits – towards highly specific adaptive deep brain stimulation

Abstract

Neuro-electronic interfaces, which can be used for stable communication between neurons-computers over long periods of time, would be valuable for understanding and interacting with the nervous system. A major challenge has been to overcome the tissue reactions towards implanted electrodes. Flexible microelectrodes that cause less implantation injury and which can follow the micromotions of the brain have been considered as a solution to achieve stable neuronal recordings and stimulations. The aim of this thesis work was therefore to develop and evaluate biocompatible neuro-electronic interfaces, as well as introduce new implantation methods which together allow stable recordings and spatially precise stimulation of the brain

To this end, we have developed a new generation of ultrathin flexible electrode arrays based on 12.5 µm thin wires embedded in a gelatin vehicle providing structural support during implantation. The gelatin embedded electrodes were implanted in rat brains via a narrow track line and spread out as a cluster in the target area. In the first study, we evaluated the performance of the neural recordings for eight weeks with respect to impedance, signal amplitudes and noise levels. We found impedance, and signal to noise ratio of single units to be quite stable, suggesting high biocompatibility. In the second study, we developed a gelatin embedded microelectrode array consisting of 16 microelectrodes, distally equipped with silicone cushions to reduce vascular damage. This array was implanted medial to the subthalamic nucleus, in 6-hydroxydopamine lesioned rats (a classical animal model for Parkinson's disease), and the effects of deep brain stimulation were evaluated for 6 weeks. Stimulation with subsets of 4-8 electrodes evoked specific motor behaviors in all the tested rats. Depending on the exact electrode combination, stimulation elicited either improvement of locomotion, or grooming and rearing, increased turning, dyskinesia, or no movement. These results suggest that improved stimulation specificity can be obtained by choosing the right group of electrodes from the cluster. In the third study, we hypothesized that reducing the tissue resistance during the insertion of the electrodes would minimize the implantation injury. To address this problem, we coated gelatin embedded needles with a layer of ice, which on melting, provided a super slippery surface during insertion into the brain. The addition of a layer of melting ice decreased the insertion force by approximately 50%, significantly reduced neuronal loss, as well as the astrocytic response, but did not have any obvious effect on microglial activation.

In conclusion, this thesis presents a novel design for implantable and biocompatible neuro-electronic interfaces comprising highly flexible microelectrodes rendering stable recording properties and improved stimulation specificity. In addition, a novel implantation vehicle was developed to reduce the acute tissue reactions in response to the implantation

Keywords: Neuro-electronic interface, neural interface, tissue reactions, deep brain stimulation, Adaptive DBS, biocompatibility, implantation method, neurosurgical tool

Classification system and/or index terms (if any)

Supplementary bibliographical information		**Language: English**
ISSN and key title. 1652-8220		**ISBN:** 978-91-7619-989-3
Recipient's notes	**Number of pages** 65	Price
	Security classification	

Signature  Date 2019-10-22

Microelectrode cluster technology for precise interactions with neuronal circuits

Towards highly specific adaptive deep brain stimulation

Mohsin Mohammed

LUND
UNIVERSITY

Cover photo by Rolf Graham, Karlshamn, 2016

Faculty of Medicine
Department of Experimental Medical Science

ISBN 978-91-7619-989-3
ISSN 1652-8220

Printed in Sweden by Media-Tryck, Lund University
Lund 2020

To my beloved Abba

Table of Contents

Abbreviations

6-OHDA	6-Hydroxydopamine
BBB	Blood brain barrier
BMI	Brain machine interface
CO_2	Carbon dioxide
DA	Dopamine
DBS	Deep brain stimulation
ED1	Antibody staining microglial cells
GFAP	Glial fibrillary acidic protein
IL	Interleukin
Ir	Iridium
NeuN	Neuronal nuclei
PBS	Phosphate buffered saline
PD	Parkinson's disease
PDMS	Polydimethylsiloxane
PEG	Polyethylene glycol
Pt	Platinum
RNS	Reactive nitrogen species
ROI	Region of interest
ROS	Reactive oxygen species
RT	Room temperature
SD	Standard deviation
SN	Substantia nigra
SNR	Signal to noise ratio
STN	Subthalamic nucleus
TH	Tyrosine hydroxylase

Popular scientific summary

Neurons communicate with each other by sending electrical signals. To understand the brain during normal conditions or during neurological disease, these electrical signals can be recorded by inserting electrodes into the brain. In some disease conditions, the electrical communication between different parts of the brain is compromised. In such cases, electrical signals can be modulated by sending electrical current from an external source, via implanted electrodes. However, currently used electrodes employed for communication with the brain are relatively large and thus cause substantial damage during implantation. Because of the injury, the brain recognises the implanted electrodes as an invading "foreign body" and sends "police cells" (glial cells) to combat the invasion. These police/glial cells progressively surround the implanted electrode, isolating it from the rest of the tissue, thus making it hard to record or modify neuronal signals stably. The size of the team of police cells surrounding the implanted electrode is dependent on the magnitude of injury, i.e., the bigger the injury, the bigger the team of police cells called in. Thus, it is important to reduce the injury and to minimize this tissue response which obstructs communication (stimulation and recording) with neurons at close range. In addition, large sized electrodes prevent precise stimulation of specific and limited target areas and will instead affect a larger volume of tissue surrounding it, e.g. resulting in unspecific stimulation of unintended neurons or neuronal signals which may in turn cause side effects. The small, and ultra-flexible microelectrode arrays has the advantages of causing less injury upon implantation into the brain due to their reduced size. The smaller injury induces recruitment of fewer police cells with less isolation of the neurons, and thus the potential for communication with surrounding neurons is improved. The reduction in size of the microelectrodes, increase their stimulation specificity, as they will only affect the neurons or neuronal signals nearby, and thus reduce the side effects due to unspecific stimulation of larger tissue volumes. In addition, flexible microwires have been put forward as a solution to achieve better integration and stability of electrodes in the tissue, and thus more stable stimulation/recordings. However, flexible microelectrodes are difficult to implant in the brain tissue, as their low stiffness make them prone to bend during implantation. This thesis was aimed at developing and evaluating micro-size electrodes and improving the methods to implant them.

We have developed a new type of brain implantable electrode array, which contains many, very thin (20 μm), microwire electrodes embedded in gelatin. In comparison, a human hair has a thickness between 50-80 μm. Gelatin, when dry, provides the necessary stiffness/support to microwires to avoid bending during implantation. In

our first study, we recorded neuronal signals from rat brain for eight weeks. The neuronal signals were of high quality, with good signal strength during the whole test period, indicating improved integration of the implanted electrodes in the tissue. In the second study, we evaluated modulation of neuronal signals, in rats with induced motor deficits (a rat model mimicking the motor symptoms seen in Parkinsonian patients), by delivering electrical current via the implanted electrode. Electrical stimulation through implanted clusters of microelectrodes was able to reduce the motor deficits in the rats, indicating that it is possible to modulate brain signals using microelectrode clusters. In addition, by selecting the specific microwire electrodes which evokes normal walking behaviour, and by not using the microwire electrodes which evoked side effects, we were able get beneficial effects with reduced side effects. Furthermore, neurons were found within <10 micrometers (1/1000 of a mm) distance of the implanted microwires, indicating reduced tissue damage and presence of neurons very close to the electrodes. The loss of neurons in the close vicinity of electrodes is a common problem which obviously impede communication with neuronal tissue. In the third study, we evaluated the tissue effects of reducing the roughness of electrodes, i.e. the surface coming into contact with the tissue during implantation. To accomplish a less rough surface, we coated gelatin needles with a super slippery coat of melting ice. The addition of a melting ice-coat reduced the force, required to insert them into the brain, by half. In addition, it reduced the loss of neurons in the insertion track, as compared to the same type of implants but without the slippery ice-coat. This indicates that a reduced force/friction inflicted on the tissue by electrodes during implantation is important to minimize injury.

In conclusion, this thesis presents a novel design of implantable microelectrode arrays containing multiple microwires, as well as a new method to implant such constructs with reduced insertion forces. The new techniques proved to minimize tissue damages and increase the stimulation specificity, thus achieving more stable and precise electrode-neuronal communication, something which is important within research as well as for treatment of neurological diseases.

Original Papers included in this thesis

This thesis is based on the following articles, which will be referred as Paper-I, Paper-II and Paper-III hereafter

Paper-I:

Etemadi. L*, **Mohammed. M ***, P. T. Thorbergsson, J. Ekstrand, A. Friberg, M. Granmo, L. M. E. Pettersson# and J. Schouenborg# (2016). "*Embedded Ultrathin Cluster Electrodes for Long-Term Recordings in Deep Brain Centers*." Plos One 11(5).

*Equal contribution, # These authors jointly directed this work.

Paper-II

Mohammed. M, N. Ivica, H. Bjartmarz, P.T.Thorbergsson, L. M. E. Pettersson, J. Thelin and J. Schouenborg. *A novel strategy and design of microelectrode based deep brain stimulation for improved therapeutic specificity and reduced side effects* (Manuscript)

Paper-III

Mohammed. M, J. Thelin, L. Gallentoft, P. T. Thorbergsson, L. S. Kumosa, J. Schouenborg, and L. M. E. Pettersson. "*Ice-coating-a New Method of Brain Device Insertion to Mitigate Acute Injuries*". Journal of Neuroscience Methods 343 (Sep 1 2020).

Introduction

History and potential of neuro-electronic interfaces

Alan Hodgkin and Andrew Huxley explained the concepts of membrane current and the mechanisms of an action potential [1]. Jose Delgado in 1965 displayed the most stunning demonstration of the power of brain stimulation when he successfully stopped a charging bull by electrical stimulation of thalamo-basal ganglia circuitry [2]. These discoveries laid the foundation for recording and stimulating of the brain, not only for functional understanding but also for therapeutic purposes.

Elwin Marg and John Adam were the first to use multielectrode arrays in humans for recordings [3]. These recording techniques became valuable tools to analyze information processing in complex neural circuitries as they allow recordings from relatively large numbers of neurons during various behavioral tasks [4]. The techniques were further improved to the point where the recorded signals can be used to control robotic arms, leading to the development of Brain-Machine Interfaces (BMI) [5]. The first breakthrough in the usage of BMI's was achieved when amyotrophic lateral sclerosis patients, with impaired voluntary movements, were able to successfully move a cursor on a computer screen via a brain implant in the motor cortex connected to a computer [6].

Neuro-electronic interfaces can also be used for chronic brain stimulation to produce symptomatic relief in untractable neurological disorders. Ugo Cerletti introduced modern-day brain electrical stimulation to treat psychosis in 1940 [7]. Heath and Mickle electrically stimulated the septal area using intracranial electrodes for controlling pain [8, 9]. Benabid et al. reported that stimulation of the ventral intermediate nucleus of thalamus ameliorated tremor in Parkinson’s diseases (PD) and essential tremor patients [10]. Pollak et.al. were able to mitigate motor akinesia in Parkinson's disease patients by stimulating the subthalamic nuclei [11]. These studies initiated and established a framework for the field of deep brain stimulation (DBS) for treating various neurological disorders. The US food and drug administration authority has approved DBS for treatment of chronic pain (1989) [12], essential tremor (1997), motor symptoms of PD (2002), and dystonia (2003) [13].

Together, the electrophysiological recording and stimulation techniques have proved valuable in both brain research and for symptomatic relief of neurological diseases. However, there are significant hurdles to overcome before neuro-electronic interfaces will reach their full potential.

Current state of the art

Implantable electrodes for neuronal recordings

Due to considerable international efforts, a plethora of microelectrodes are currently available for recordings of neuronal signals [14, 15]. The most commonly used electrodes for recordings can be broadly divided into three types briefly described below.

Metal wire electrodes

Metal wire electrodes are one of the simplest and most commonly used type of recording electrodes, and it's usage dates back to the early twentieth century [16]. Such electrodes consist of an insulated, electrically conductive wire with a diameter in the range of 25-75 μm and can, due to their stiffness, be inserted into soft tissue without structural support. While useful for many applications, there are well known problems with deterioration of electrode performance over time, probably due to their relative stiffness causing tissue reactions (see below). More recently, ultrathin and therefore highly flexible wire electrodes embedded in stiff gelatin providing structural support during implantation, have been introduced for cortical recordings showing very promising results with respect to signal quality and stability [17, 18]. To meet the need to record from many neurons simultaneously, current efforts are, to a large extent, directed towards development of multichannel devices, comprising microwire bundles or arrays held together by connectors or printed circuit boards [19-21]. One potential disadvantage of the multichannel microwire-based electrodes is that manual assembly of wire electrodes has hitherto been necessary, leading to reproducibility problems and reduced production capacity. Nevertheless, ultra-flexible wire electrodes remain an interesting option also in the future, if effective manufacturing can be achieved.

Micromachined microelectrodes

Photolithographical methods are used to microfabricate a pattern on a photoresist polymer that can be transferred into the underlying substrate by chemical etching [22-25]. The invention of photolithography led to the development of a new generation of neural electrodes. Various designs and shapes in two or three dimensions of neural interfaces have been manufactured using micromachining/photolithography techniques and have been tested in experimental animals with variable success [26, 27]. The Michigan electrode array and the Utah electrode array are typical examples of electrodes fabricated using micromachining techniques [28, 29]. Micromachining has undoubtedly enhanced the reproducibility of the manufacturing process, and also improved the ability to record from a larger number of neurons. However, stable long-term recordings, from the same neurons over time, are usually not obtained with such electrodes, indicating poor positional stability in the tissue and/or low biocompatibility[30].

Thin-film polymer-based microelectrodes

Thin-film polymer-based electrodes are made by sandwiching metal between layers of polymeric substrates like benzocyclobutane, polyamide, polydimethylsiloxane (PDMS), parylene, etc. The polymer layers (< 10 μm thickness) are used as the base material. Conductive materials, such as Au, Pt, or Ir are deposited on the polymer base either by sputtering or evaporation. Polymer-based electrodes are quite flexible and overcome to some extent the disadvantage of stiffness, thereby increasing biocompatibility by reducing tissue inflammation [30-32]. However, the insertion of such ultra-flexible electrodes into soft tissue requires some form of structural support, which can cause injuries and when extracted may dislocate the implanted electrodes [17, 31, 33, 34]. Moreover, it is not entirely clear whether these electrodes remain stably positioned in the tissue after implantation [35, 36].

Implantable electrodes for electrical stimulation

Although electrodes for recordings can also be used to stimulate nervous tissue, their small contacts, necessary for recording neuronal signals, permit only very weak stimulation currents to be safely delivered. To be able to deliver sufficient current for inducing noticeable behavioural effects or therapeutic effects, electrodes used for stimulation tends to be much larger than those for recordings. Typically, stiff metal electrodes with a diameter in the range of 50-100 μm are used for brain stimulation in rodents and non-human primates.

In the clinic, the size of the electrodes and contacts used are in the millimetre scale [37], which limits possibilities for spatially precise stimulation. In comparison to

the development of recording electrodes, little development has been made with regards to stimulation electrodes [38] . However, more recently, several novel designs with more electrode contacts have been developed and are being tested to improve the control of current spread in the tissue ("Model 6180" by Abbott, "Cartesia" by Boston Scientific)[39]. However, the individual electrode contacts are still placed on the same physical entity, which limits the precision of spatial stimulation.

Tissue reactions to implanted neuro-electronic interfaces

A common problem of all electrodes is that the tissue react to the implanted foreign body in a complex, and still not fully understood, way [40]. These reactions can be broadly divided into two main categories: i) reactions due to acute injuries caused by the insertion procedures and ii) tissue reactions to the implanted object.

Insertion induced tissue reactions

The insertion of a neuroelectronic interface into the brain causes variable degrees of physical tearing of the tissue, thereby rupturing connections between neurons, glia cells, and also of blood vessels which results in a breach of the blood brain barrier (BBB) [41]. Rupture of blood vessels likely create an ischemic milieu in the vicinity of the implant, which may be harmful to neurons which are critically dependent on a constant blood supply [42, 43]. Moreover, the rupture of the BBB contributes to local increase in haemoglobin from degraded red blood cells, leading to an increase in reactive oxygen species (ROS) and reactive nitrogen species (RNS) [44, 45]. Increase in ROS and RNS may, in turn, cause secondary damage by oxidation of lipids, proteins and by inducing upregulation of proinflammatory cytokines [44, 46]. Force measurements also show that significant forces, termed residual forces, possibly introduced through dimpling of meninges and friction between the implant surface and tissue, persist for a long time after completion of the insertion [47, 48]. Therefore, there is a need for development of improved insertion methods reducing friction during implantation.

Acute and chronic foreign body reactions

After implantation, neighbouring microglia rapidly extend their processes towards the injury [49-51]. These activated microglial cells begin to encapsulate the implant with lamellipodia within 30 min and release proinflammatory cytokines such as

interleukins (IL-α,1IL-1β, IL-6) [49, 52, 53]. Additional microglial cells and macrophages are mobilized after release of ILs [54]. Within roughly one day, the microglia transforms into a mobile stage and their cell bodies begin to travel towards the implant forming a thin layer, ensheathing the implant [55], which directly affects the communication potential of the implanted neuroelectronic interface. Thereafter, astrocytes proliferate around the implant and usually form a dense capsule around the microglia sheath within 1-3 weeks. The astrocytic encapsulation limits the flow of ions in the area [56], leading to increased impedance and a decline in recording and stimulation quality [57, 58] which further hinders communication between the implant and neuronal tissue. In addition to the acute and chronic inducers of the foreign body response mentioned above, micromotions between the implant and tissue further aggravates the glial reactions [35, 59]. Micromotions arise due to mechanical mismatch between the electrode and tissue during pulsating blood flow, breathing movements and also movements of the body [35]. It is thus of importance to reduce micromotions, to achieve effective integration of implanted devices and improvement of the electrochemical signaling at the electrode-tissue interface. Recent studies have shown that the formation of glial encapsulation and the ubiquitous loss of neurons nearby can be substantially mitigated by increasing the flexibility and reducing the weight of the microelectrodes, as well as by coating/embedding the microelectrodes in gelatin [17, 59-64]. While these and other studies have focused on implantation into cortical (more superficial) tissue, there is a lack of neuro-electronic interfaces that can be precisely implanted in deep brain tissue and reside stably in the tissue.

Parkinson's disease and Deep Brain Stimulation

A common clinical application for DBS is for treatment of symptoms of PD. PD is the second most common neurodegenerative disorder. It is caused by the loss of dopaminergic neurons in Substantia Nigra (SN) pars compacta, and is characterized by slowness of movement, rigidity, postural abnormality, and tremor [65-68]. Dopamine (DA) replacement using the DA precursor levodopa is still the golden standard treatment for relieving the motor symptoms of PD [69, 70]. However, in later stages of PD, one-third of patients treated with levodopa develop motor fluctuations and dyskinesia, which substantially decrease quality of life [71-73]. These patients can still benefit from DBS in the basal ganglia region [74].

However, while current DBS can effectively restore motor functions in PD in many cases, side effects like gait ataxia, speech disturbances, behavioural changes like aggression, depression, and restlessness, changes in blood pressure, and paresthesia

are frequently reported [75-77]. The adverse effects are assumed to be, at least partly, due to spread of current to undesired areas within or outside the stimulated nuclei, which is in turn due to the large size of the currently used electrodes [78, 79]. Other reasons for the adverse effects of DBS include the size of the injury caused by implantation, inaccurate choice of stimulation parameters, and the inability of rigid electrodes to follow micromotions of the brain. All these factors, can cause tissue reactions, which in turn lead to inflammation, astrocytic responses and microglial activation [80]. Notably the scarring around an implanted DBS electrode may extend almost a millimetre from the electrode surface which has a diameter of 1.2–1.4 mm [81, 82]. Thus, there is a need for developing miniaturized neuroelectronic interfaces which can stimulate locally and also reduce implantation induced injury and tissue reactions. However, as mentioned above, single microelectrodes may not suffice to provide therapeutic effects. A conceivable approach is therefore to make use of multiple microelectrodes that together can provide efficient stimulation.

Aims of the thesis

The purpose of this thesis was to develop novel biocompatible neuro-electronic interfaces, and implantation methods, which allow stable recordings and spatially precise stimulation of the brain. The specific aims were to:

1. Develop a novel gelatin embedded array of microelectrodes, for deep brain recording and stimulation, and evaluate its electrophysiological and biocompatibility properties.
2. Clarify if multichannel microelectrode based micro-stimulation can be used to obtain high stimulation specificity and to reduce stimulation-induced side effects.
3. Evaluate a novel low-friction insertion vehicle with respect to implantation induced brain trauma and acute tissue reactions.

Methods and rationale

A brief description of the methods will be given in the following sections. Please refer to the individual studies (appendix) for a more detailed description of methods. The Malmö/Lund animal ethics committee on animal experiments pre-approved all the animal experiments. Adult female/male Sprague-Dawley rats weighing about 200-250 g were used. Animals received food and water ad libitum and were kept at a controlled environment of 21ºC and 65% relative humidity, 12-hour day-night cycle. In Paper-III, the day-night cycle was reversed for the animals.

Electrode bundles embedded in gelatin

In Paper-I, we used bundles of 29 platinum (Pt) wires (Advent Research Material, England), with an individual wire diameter of 12.5 µm plus an insulating layer of parylene C (4 µm). To enhance the quality of soldering, the proximal ends of the Pt wires were de-insulated and gold plated before soldering them to the gold plated pads of the printed circuit board. For recording purposes, the distal parts of the electrodes were de-insulated (25 ± 5 µm from the distal end), using a UV laser (wave length 355nm, energy density 1.89 J/cm^2) (Standard micro-milling system, New Wave Research Class 1, USA). To decrease the impedance of the recording sites, the effective surface area of the recording sites was enhanced by briefly exposing them to high power UV laser (wavelength of 355 nm, energy density 6.9 J/cm^2). The microwires were then embedded in gelatin by slowly dipping (1.2 cm/min) in a solution of 27.5% gelatin (120 Bloom strength, VWR international, Sweden), 6.9% polyethylene glycol 400 (PEG) (Sigma-Aldrich Chemie GmbH, Germany), and 1.4% glycerol (VWR, BDH Prolabo, France) dissolved in deionized water. Glycerol and PEG were added to create a smooth surface of the gelatin probe and to reduce tendencies to bend during drying. Finally, the electrode bundle was placed in a mold, and additional gelatin solution was injected through a side-channel to form a probe with a stiff shaft and a conical tip. The construct was allowed to slowly dry at room temperature (RT), 21% relative humidity. To delay the dissolution time of gelatin when inserted into the brain, the shaft of the gelatin probe was dip-coated (speed 6 cm/min) with two layers of 5 % Kollicoat TM MAE 100P (Sigma Aldrich

Sweden AB) dissolved in absolute ethanol. An un-insulated silver wire (150 µm in diameter, Advent research material, UK) was soldered to the PCB and served as animal ground.

In the second study (Paper-II), preceded by extensive pilot testings, a number of adjustments of the gelatin techniques and also of the microelectrodes themselves were introduced. Medical grade gelatin (Gelita, Medella Pro 1500, USA) was used without any additives. Bundles consisting of 16 Pt/Iridium (Ir) alloy (90% Pt/10% Ir) wires with a diameter of 12.5 µm (California Fine wires, USA), insulated with 4 µm layer of parylene C, were used. The assembly of the probe is outlined in Fig. 1. The distal part of the wires was de-insulated for a length of 600 µm by focused low power UV laser (wave length 355 nm, energy density 1.89 J/cm^2) and then briefly exposed to high power UV laser (wave length 355 nm, energy density 3.3 J/cm^2) to create a roughened contact surface with low impedance. The microwires were then cut at both ends, and the proximal ends (to be attached to the contact) were de-insulated using a butane flame and pre-tinned to facilitate soldering.

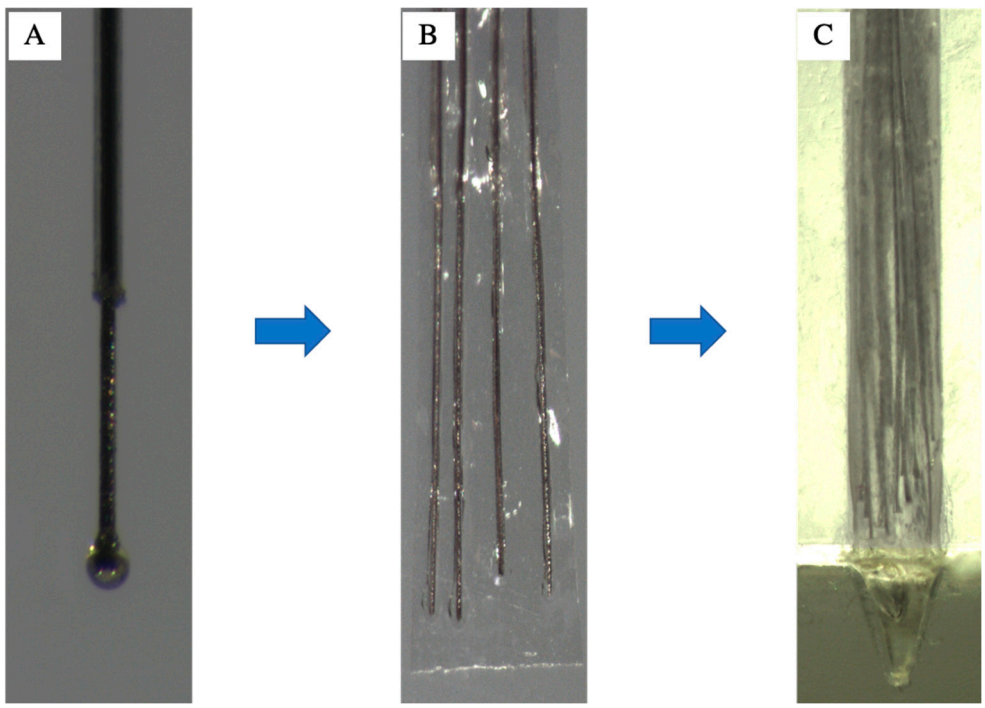

Fig. 1. Various steps in development of a microelectrode probe. (A) Pt/Ir single microwire (diameter 12.5 µm) insulated with Parylene C. The distal end of the wire is de-insulated 600 µm, and has a silicone cushion at its tip. (B) Gelatin flake containing four microwires (C) Four flakes stacked together and molded in gelatin to produce a 16 microelectrode cluster array. Reprinted (adapted) with permission from Paper-II.

Silicone cushions in a range of 50-100 µm were manually attached to the distal part of the electrodes under a microscope. The silicone cushions were added to minimize the risk of tissue injury and puncturing of blood vessels during insertion of the microelectrodes. After curing the silicone, the microwires were dipped in 30% gelatin solution (289 Bloom strength) at 50ºC to a length of 1500 µm from the distal end.

Groups of four gelatin dipped microwires were aligned in parallel, using a fine brush and 90% ethanol, on an non-adherent plastic surface (Polypropylene copolymer, Gillbert Curry Industrial Plastics Co Ltd, UK) for a length of 1 cm from the distal end. The aligned microwires were kept on dry ice for 20 min and then sprayed with 10%, 50ºC low Bloom gelatin (101 Bloom strength) using an airbrush (Iwata gravity feed dual-action airbrush, Anest Iwata-Medea Inc, Portland, USA), to create frozen flakes of gelatin (Fig. 1B) fixating the wires. The gelatin flakes were allowed to dry at RT for 1h and then removed from the polypropylene sheet. Four gelatin flakes were stacked and aligned in custom-made plexiglass molds (Prototech AB, Helsingborg). Gelatin, 30% (101 Bloom strength) at 50ºC, was injected into the mold for embedding the stacked electrode flakes and allowed to slowly dry at RT with 50% relative humidity in a temperature and humidity-controlled chamber (Rcom, Kingsuro Max 20 digital Incubator). The non-embedded proximal de-insulated tips were soldered to 16 pins on a male Omnetics connector (Plexon, CON/32m-VA8828-001, USA) under a stereomicroscope (Olympus, Szx7 0.5-4X, Japan). A non-insulated Pt wire (25 µm, PT005114, Goodfellow Cambridge Ltd, UK) was soldered to a pin dedicated to ground on the Omnetics contact and served as animal ground during stimulations. The proximal parts of the electrodes and the animal ground wire, along with the un-insulated pins of the contact board were then covered with Epoxy (Epoxy Technology, Epotek OG198-54 and 55, USA) and cured with UVB light (Honle, Blue Point Eco Led, Germany). Finally, the electrode bundle was removed from the mold and stored at -20 ºC until implantation.

Gelatin embedded needles

In Paper-III, stainless steel needles (diameter 100 µm) were embedded in 30% gelatin (101 Bloom strength, Gelita, Medella Pro 1500, USA) dissolved in de-ionized water, using custom made molds (inner diameter 350 µm). The gelatin embedded needles were allowed to dry at RT for four hours followed by drying in a vacuum chamber for six hours. One group of gelatinized needles were frozen on

dry ice and then dipped twice in 4ºC de-ionized water to form an ice-coat. The ice-coating of the gelatinized needles was done just before implantation surgery.

Anesthesia and Surgery

Surgeries were done under deep anesthesia. Types of anesthesia used in Paper-I, -II and -III are outlined in Table.1. After shaving the rats´ head, the animals were mounted in a stereotactic frame and a midline incision was made. Connective tissue, bone and dura mater were removed thus exposing the cortical surface.

In Paper-I, the implantation of the electrode array was done in three steps: i) insertion of the probe to pre-target (1 mm above target) with a speed of 100 µm/s, ii) waiting for 10 min allowing swelling of gelatin to separate the microwires and iii) slow insertion (10 µm/s) into the target area.

Table.1. Summary of the types of anesthesia used in Papers I, II and III

	Implantation Surgery	Neuronal recording	6-Hydroxydopamine lesions
Paper -I	Fentanyl (0.3 mg/kg) + Medetomidine hydrochloride (0.3 mg/kg)	A mixture of 1% Isoflurane, 30-40% oxygen, 60-70% nitrous oxide	Not applicable
Paper-II	A mixture of 1.2-2 % Isoflurane, 30-40% oxygen, 60-70% nitrous oxide	Not applicable	Fentanyl (0.3 mg/kg) + Medetomidine hydrochloride (0.3 mg/kg)
Paper-III	A mixture of 1.2-2 % Isoflurane, 30-40% oxygen, 60-70% nitrous oxide	Not applicable	Not applicable

In Paper-II, a unilateral lesion of dopaminergic neurons were made by injecting 6-Hydroxydopamine (6-OHDA; 3-3.5 µg dissolved in 0.02% ascorbic saline) in the medial forebrain bundle [83]. The animal was then allowed to wake up and recover. Two weeks later, the electrode probe was implanted using a robotic stereotactic instrument (Neurostar, Robot Stereotaxic instrument, Germany). A faster three-step insertion procedure, guided by preceding *in vitro* tests in saline, was used as compared to that in Paper -I, and comprised: i) insertion of the probe to pre-target (3mm above target) with a speed of 1 mm/sec, ii) waiting time of 4 min, and iii) slow insertion (50 µm/s) to the target area.

In Paper-III, four stab wounds were made, two in each hemisphere, using gelatin coated stainless steel rods with or without a coat of ice: The needles were inserted

into striatum to a depth of 5 mm with a speed of 1000 µm/s. After a waiting time of 10 min, the central, stainless steel rod was retracted at a speed of 100 µm/s.

Characterization of electrodes in vivo

In Paper-I and -II, *in vivo* electrical impedance was regularly measured at 1 kHz frequency for 6-8 weeks either using a Plexon stimulator 2.0 (Paper -I, Plexon Inc, Texas, USA) or a NanoZ impedance tester (Paper-III, Plexon Inc, Texas, USA). This was made to assess the integrity of the implanted electrodes and the stability of the electrode-tissue interface.

In Paper-I, extracellular electrophysiological signals were acquired in anesthetized rats, starting 1-day post-implantation. The implanted probes were connected to the Plexon acquisition system (Plexon Inc, Texas, USA) via a head stage connected to a pre-amplifier. The acquisition of neuronal recordings was made once per week for up to 8 weeks post implantation. A band-pass filter (250-8000 Hz), excluding low frequency local field potentials, was used for neuronal recordings. Spike detection was performed by applying a negative threshold equivalent to four times the estimated noise level of the bandpass-filtered signals. Noise level estimation was performed by using median absolute deviation (MAD) estimator, given by:

$$\sigma_N = \frac{median(|v(n)|)}{0.6745}$$

where σ_N is the estimated noise level and $|v(n)|$ is the absolute value of the band-pass filtered signal. Detected spike-waveforms were sorted using principal component analysis (PCA) for feature extraction and Gaussian mixture models (GMM) for clustering [84].

The signal to noise ratio (SNR) of single units was calculated as peak to peak amplitude divided by twice the standard deviation of the residuals of spike waveforms after subtracting the mean waveform.

Behavioural tests

In Paper-II, we evaluated the effects of DBS on motor behavior in 6-OHDA lesioned rats using the open field setting and limb use asymmetry/cylinder tests.

Open field

An open-field setting (essentially a container of 80x80 cm) was used to assess exploratory behavior and general activity level before and during DBS. The animal's movements were monitored using a camera (Logitech HD pro webcam c920, Logitech Inc), and a head-mounted 3D-axes accelerometer (ADXL337, Analog devices Inc.). An in-house developed program in Matlab (MATLAB, 2019, Natick, Massachusetts: The MathWorks Inc., 2019) was used to analyze the animal movements offline. Two LEDs (blue towards nose and red towards neck), were mounted on the accelerometer attached to the rat's head stage, permitting recognition of the head-position and direction of movement. The total displacement of the head after stimulation-onset was taken as the displacement of the rat.

Limb use asymmetry/cylinder test

In the cylinder test, the rat was put in a clear glass cylinder (40 cm high and 20 cm wide), and as the rat explores and leans against the cylinder wall, the number of touches using the left or right paw were counted and used to quantify usage symmetry. Mirrors were mounted behind the cylinder test to facilitate the visibility of the rat from all sides. The test was video recorded and counting of usage of left and right paws was done offline using an in-house developed software in Matlab (MATLAB, 2019, Natick, Massachusetts: The MathWorks Inc., 2019). To evaluate the effects of DBS on limb use asymmetry, the cylinder test was performed both with stimulation off and stimulation on.

Deep brain stimulation protocol

DBS was performed using an implanted 16 channel electrode array connected to a constant current Plexon stimulator (Plexon Inc, Texas, USA) via an Omnetics connector, and a commutator which allow unrestrained animal movement. The experimental protocol for the 6-weeks DBS evaluation is outlined in Fig. 2. Stimulation was performed once a week, using biphasic charge-balanced pulses with a pulse width of 60 μsec and a frequency of 160 Hz. All stimulations were

controlled via programs written in Matlab (MATLAB, 2019, Natick, Massachusetts: The MathWorks Inc., 2019).

For identifying optimal parameters for stimulation current, all working electrodes in the probe were initially stimulated simultaneously with increasing current intensities in steps of 2 µA starting from 10 µA. The lowest current power, at which clear changes in motor behavior were evident, was taken as the base threshold current.

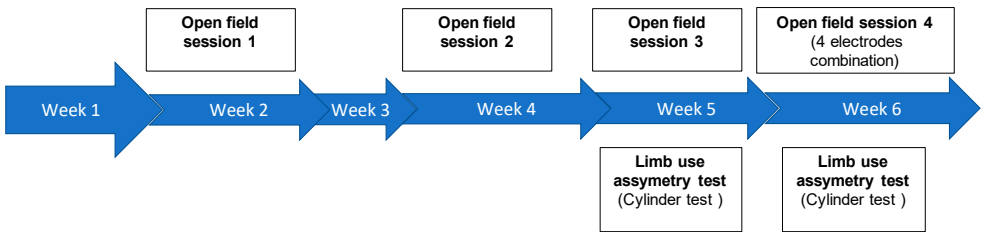

Fig. 2. Experimental design and timeline followed during DBS expirement for each rat. Search strategy-I, to find the most effective electrodes, was evaluated in open field session 1, 2 and 3 using combinations of eight active electrodes. In addition, synergetic effects, of using multiple electrodes, on threshold current were evaluated in session 1-3. Search stratergy-II, to find the most effective electrodes, was evaluated in open field session 4, where combinations of four active electrodes were tested. During week five and six, effects of stimulation on limb use assymetry were evalauted in cylinder tests. Reprinted (adapted) with permission from Paper-II.

Strategy-I

To determine which combinations of electrodes improves the motor behavior, 26 combinations (out of 12870) of 8 electrodes were arbitrarily defined, such that each electrode was included an equal number of times. The stimulation current was fixed to 1.1 times the base threshold current. Real-time monitoring of rat movements was performed using a head-mounted accelerometer and video tracking of the LEDs attached to the head stage of the animal. Stimulation commenced automatically when the head-mounted accelerometer detected no movement for 1 sec. The stimulation continued for 10 sec, then the software automatically stopped the stimulation and continued to the next combination. The software automatically determined the displacement score for each electrode in a given session using video tracking of the LEDs attached to the accelerometer on the rat´s head stage. Based on the summed displacement scores, resulting from the 26 combinations, the electrodes reaching the highest total scores were determined.

Synergy testing

For evaluating the synergy effects of increasing the number of active electrodes (from one to four) on the threshold current per electrode, we started by using the highest ranked electrode and increased the current in steps of 2μA starting from 10 μA until apparent changes in motor behavior were observed. Following this, the initial current was decreased to 10 μA, the second-highest ranked electrode was added, and the current was again increased until apparent motor behavioral changes were observed, and so on.

Strategy-II

In a second search strategy to determine which combination of electrodes was most efficient in inducing motor behavior, 42 (out of 1820 possible) combinations of four active electrodes were used and displacement scores were calculated. The combination was selected in such a way that each electrode was used 10-11 times for stimulation. The stimulation current was kept at 1.1 times the threshold current found during the synergy test using four electrodes.

Limb use asymmetry test/ Cylinder test

Baseline testing (for 2 min) with no stimulation was done at the start of the cylinder test. After that, the stimulations were delivered using the four electrodes, with the highest displacement scores in open field tests (Strategy-I). The stimulation current used was the average threshold current found in synergy testing. In the events where a symmetry of paw usage was not reached, the stimulation current was ramped up in steps of 3μA. In the second cylinder test, the stimulations were delivered using the four electrodes which got the highest displacement scores in the four-electrode combination open field (week 6, see Fig. 2).

Insertion force measurement

In Paper-III, the insertion force during implantation was compared between gelatin embedded stainless steel needles with or without a coat of thawing ice. Insertion forces were measured using a Micro Load Cell (0-100g, CZL639HD), in combination with a PhidgetBridge 4-Input analog-to-digital USB interface (both from Phidgets, Inc., Canada), attached to the micromanipulator.

Histology

Tissue preparation

Rats were killed by an overdose of sodium pentobarbital after 8 weeks (Paper-I), 6-8 weeks (Paper-II), 1 and 7 days (Paper-III) post-surgery. After confirmation of loss of reaction to a painful stimulus, transcardial perfusion, with 80-150 mL of 0.9% saline, was performed. This was followed by 300-320 mL of ice-cold 4 % paraformaldehyde (PFA) in 0.1M phosphate buffer, pH 7.4 and finally with 80 mL of saline prior to dissection of the brains. The brains were subsequently cryoprotected in 20% sucrose solution, snap-frozen and sectioned using a cryostat (Microm HM 560, Microm GmbH, Walldorf, Germany). The sections were 30 µm thick coronal sections in Paper-I and 16 µm thick horizontal sections in Paper-II and -III. The sections were mounted on glass slides (Super Frost plus, Menzel-Gläser, Germany).

Staining of the tissue

Nissl staining, using cresyl violet, was performed to evaluate the location of the electrodes (Paper-I). Immunohistochemical fluorescent staining was performed to examine neuronal density (NeuN staining Paper-II and -III), microglia activation (ED-1 staining Paper-II and -III), astrocytic response (GFAP-staining Paper-II and -III), and changes in blood vessel distribution (RECA staining, Paper-III). The sections were also evaluate with regards to the extent of the 6-OHDA lesion (Tyrosine hydroxylase (TH) staining, Paper-III).

Cresyl violet staining

Tissue sections were recovered from the freezer, air-dried and immersed in ethanol/chloroform (1:1) overnight, followed by rehydration through baths of decreasing concentrations of ethanol (100%, 95%, 2 min). After washing the sections in distilled water, the sections were stained with cresyl violet (Sigma) for 5 min (0.1% in 0.3% acetic acid in destilled water, Life Science products & services company), after which sections were rinsed in destilled water and dehydrated through increasing concentrations of ethanol (95% and 2x100% ethanol, 5 min/bath) and xylene (2x, 5 min). Finally, the slides were coverslipped using DPX mounting media (Fluka, Germany).

NeuN, ED1, GFAP and RECA staining

Defrosted sections were rehydrated in phosphate-buffered saline (PBS, 3 x 10 min), followed by blocking for 60 min with 5% normal goat serum in 0.25% Triton X-100 in PBS to avoid nonspecific binding of antibodies. After the blocking step, sections were incubated at RT overnight with primary antibodies (see Table.2., for list of antibodies). This was followed by rinsing the slides in PBS and incubation with the secondary antibodies goat anti-rabbit Alexa 594 (1:500, Invitrogen, USA) and goat anti-mouse Alexa 488 (1:500, Invitrogen, USA) for 2h at RT in light sealed containers.

Table.2. Summary of primary antibodies used in this thesis.

Antibody	Host	Expressed in	Clonality	Dilution	Supplier
NeuN	Rabbit	Neurons	polyclonal	1:500	Abcam, USA
Anti-CD68/ ED1	Mouse	Activated microglia	Monoclonal	1:250	AbD Serotec, UK
GFAP	Rabbit	Astrocytes	Polyclonal	1:5000	Dako, Denmark
RECA	Mouse	Endothelial cells lining blood vessels	Monoclonal	1:1000	Bio-Rad, UK
TH	Rabbit	Dopaminergic neurons and neurites	Polyclonal	1:1000	Pel-Freez, USA

Finally, all slides were rinsed in PBS and coverslipped using polyvinyl alcohol mounting media with 1,4-diazabicyclo [2.2.2] octane (PVA-DABCO, Merck /Sigma Aldrich, Sweden). The slides were stored at 4^{o}C until analyzed.

TH staining

Evaluation of TH staining was performed to determine the extent of the 6- OHDA lesions. Sections were allowed to defrost, washed in PBS (3x 10 min), and then endogenous peroxidase activity was quenched by application of 0.3% hydrogen peroxide for 15 min. After this, sections were rinsed in PBS, subsequently blocked with 5% normal goat serum in 0.1% Triton X-100 in PBS for 60 min, and incubated with primary antibody (See, Table.2.) overnight in the fridge. The following day, sections were rinsed in PBS, incubated with a biotinylated goat-anti-rabbit secondary antibody for 1 h (1:200, # BA-1000, Vector Laboratories, USA) at RT, again rinsed in PBS, and incubated with VECTASTAIN Elite ABC Reagent in PBS (avidin-biotin-HRP complex; Vectastain™ ABC Elite kit, #PK-6100, Vector Laboratories, Burlingham, CA) for 1h at RT. After this, sections were rinsed and

the antigen-antibody reaction was visualized using 3,3' diaminobenzidine (DAB Peroxidase substrate kit, #SK-4100, Vector Laboratories, USA). Finally, slides were rinsed in distilled water and coverslipped using PVA-DABCO.

Image acquisition and analysis

Images were acquired using NIS-Elements BR software and a Nikon camera (DS-Ri1) mounted on a Nikon microscope (Eclipse 80i). Images were photographed at 10x and 2x and the settings for the gain, contrast and exposure time were kept constant, for each specific marker within the separate studies, to enable comparisons.

In Paper-I, light microscopy images were taken to confirm the location and examine the spread of the electrodes. In Paper-II, the tissue was screened along the depth of the electrode array, and images were captured within the electrophysiological active depth range (stimulation site, 100-500 µm from the distal end of the microwires) to assess the effects of implanted electrodes on the tissue. The proximity of neurons to single wires was measured, changes in RECA and GFAP response were examined and quantification of microglial activation around single microwires was performed by measuring the thickness of the ED-1 immunoreactive ring around the wires.

In order to quantify the extent of the 6-OHDA lesions, low magnification images of the whole section were obtained using an Olympus camera (SDF PLAPO 1X PF, Olympus corporation) connected to a microscope (Olympus SZX2-TR30, Olympus corporation). NIH ImageJ software was used to measure the optical density of TH fibers in the striatum. The corpus callosum in which TH-positive fibers are absent was used as background. This background was subtracted before calculating the variations in staining between the lesioned and non-lesioned side and the data is presented as the proportion of TH loss on the lesioned side compared to the non-lesioned side.

In Paper-III, images from sections in cortex (900-1300 µm depth) and striatum (3500-4200 µm depth) were captured. Neuronal density (NeuN density) was evaluated in regions of interest (ROIs) beginning from the center of the insertion; i) ROI 1 = 0–75 µm, ii) ROI 2= 75–150 µm, iii) ROI 3 = 150−250 µm, and iv) ROI 4 = 350−450 µm (ROI 4 was located distantly from the stab injury and used for normalization of the neuronal density). The NeuN detection limit was set at 3.3 times the mean background intensity. The neuronal density was expressed as the fraction of NeuN stained area above threshold in relation to the total ROI area. To determine the extent of neuronal loss at the insertion site, the area devoid of neurons (neuronal void), in relation to this location, was encircled and measured.

For microglia (ED1) and astrocytic (GFAP) staining, pixel intensity-profiles were calculated using software written in Matlab. The pixel intensity-profiles along the 36 lines, 450 μm long, radiating symmetrically from the center of the stab wound, were calculated and averaged for each captured section. The data was binned into four ROIs and normalized as described above for neuronal density estimation, with the exception that the fourth ROI was moved further out to make sure that it was not affected by any injury induced glial reaction. In sections containing part of a ventricle inside the ROI, the ventricular area was subtracted from the quantified ROI area.

For comparisons between the groups, the data was normalized to ROI 4, but for comparisons within the gourps, i.e. between ROI 1-3 and ROI 4, non-normalized data was used.

Statistics analysis

In Paper-I, all the comparisons were performed using the Mann-Whitney U test in Matlab. GraphPad Prism 8.1.2 software (GraphPad Software Inc., USA) was used to perform analyses in Paper-II and -III. In Paper-II, one-way Anova with Tukey's multiple comparisons was used for all comparisons. In Paper-III, the Friedman test with Dunn's multiple comparisons was used for comparing ROI 1, 2 and 3 with 4. For comparing cold with RT or ice-coat, in Paper-III, either Friedman (where matching values were present) or Kruskal-Wallis (where matching values were missing) tests with Dunn's multiple comparisons were used. For comparison of insertion force measurement, Student's t-test was employed. P-value < 0.05 was considered statically significant.

Results and Comments

Development of a novel probe for deep brain recording and stimulation

One of the primary aims of this thesis was to develop a novel flexible neuroelectronic interface with improved biocompatibility for achieving stable recordings and increased stimulation specificity. To this end, we developed a technique that involves embedding very thin, flexible microelectrodes in a dissolvable gelatin needle, providing the required mechanical support to reach the target tissue for recording (Paper-I) and stimulation (Paper-II). Before reaching the target area the insertion was paused in a pre-target area to let the gelatin body swell and to separate the microelectrodes before advancing the last distance to the target. This novel implantation procedure allowed implantation of all microelectrodes through a relatively narrow track and subsequent separation into a cluster in the target area. The procedure was calibrated *in vitro* by implanting the probe in an agarose gel (0.5% in distilled water) and then the same insertion parameters were used *in vivo* (Fig. 3A, B). To reduce the risk of injuring the tissue and puncturing the blood vessels during insertion, we added silicone cushions to the distal ends of the microwires in Paper-II (Fig. 1A).

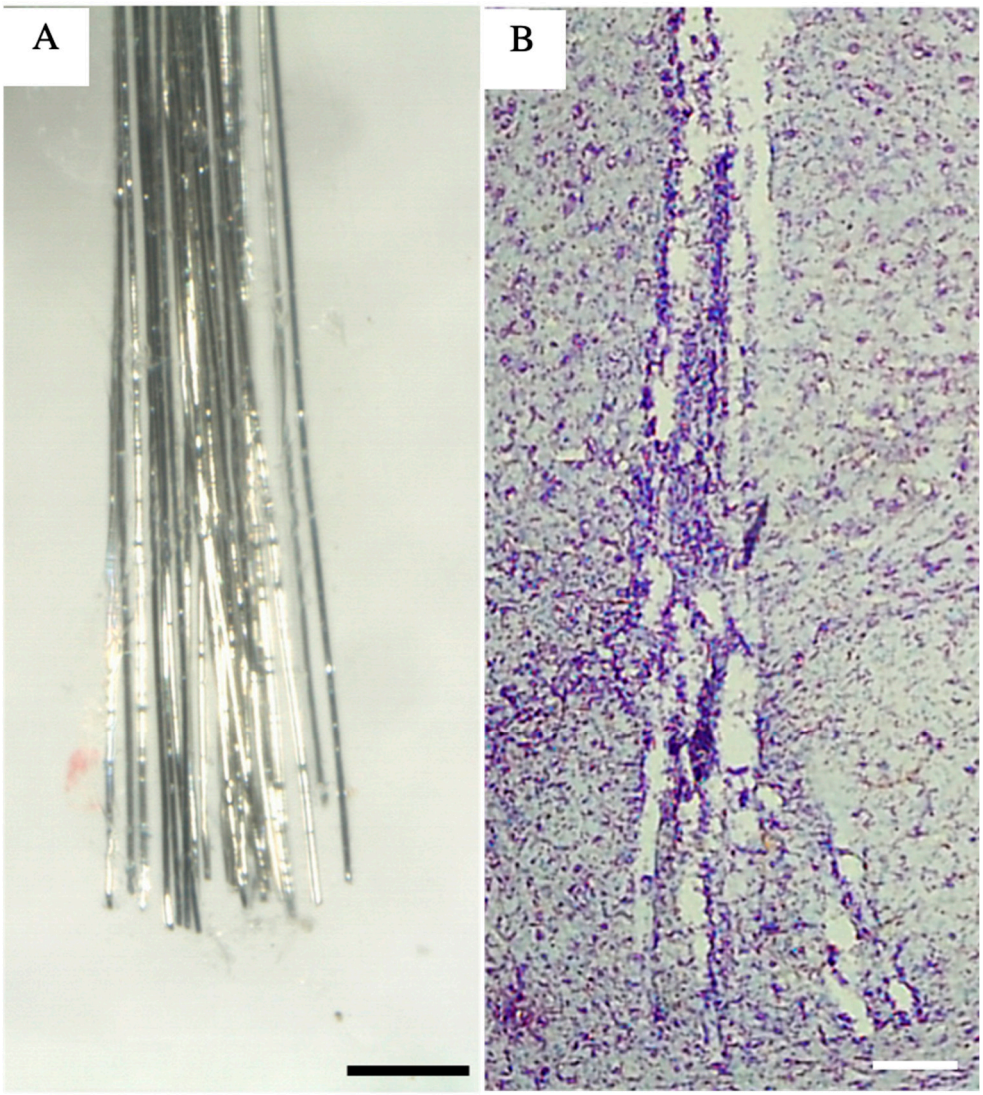

Fig. 3. Light field image of the spread electrode array in agarose (*in vitro)* and in the tissue showing the narrow track-line and spread of the array in the target area (*in vivo*). (A) Spread of individual microelectrodes after implanatation in agarose at 37°C (B) Cresyl violet staining of a brain tissue section visualizing spread of microelectrode tips *in vivo*, (Scale bar: A= 250 µm, B=200 µm). Reprinted (adapted) with permission from Paper-I.

Assessing the quality of deep brain recordings

We analyzed the quality of neuronal recordings of the developed probe (Paper-I) *in vivo* with respect to noise levels, impedance and signal to noise ratio of single units for 6-8 weeks (Fig. 4). Over the entire recording period, we were able to get high-quality neuronal recordings with multiple single units from some of the electrodes (Fig. 4A). As shown in Fig. 4B, while the median noise level increased significantly over week 1-4 (from about 4 to 8 µV), the median signal to noise (SNR, 2.77 with 1.50 IQR) (Fig. 4C) and median impedance (Fig. 4D) (median 276 kΩ, IQR= 522 kΩ) remained stable. Hence, signal amplitudes increased over time. Together these findings suggest a progressive normalization of the tissue around the implanted microelectrodes.

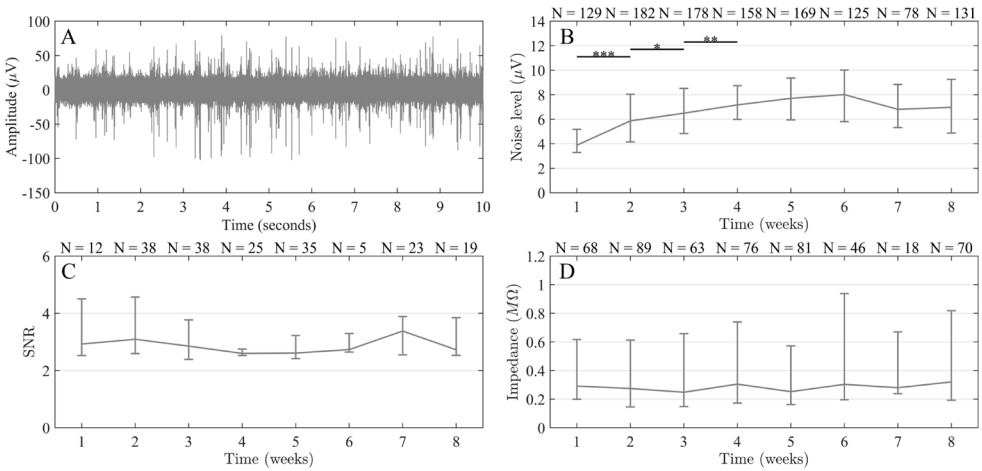

Fig. 4. *In vivo* characterization of electrode performance. (A) Typical sample of neuronal recordings (band pass filtered). (B) Distribution of noise levels (median and interquartile range (IQR) throughout the recording period (N= total number of working channels). (C) Distribution of SNR (median and IQR) of recorded channels (N= number of channels) with identified single units. (D) Distribution of impedance (median and IQR) of recorded channels (N= the number of working channels on which impedance was measured each week). The difference in N of (B-D) is largely due to a difference in number of animals recorded per week. * =p<0.05, ** =P<0.01, *** =P<0.001. (Mann-Whitney test).. * =p<0.05, ** =P<0.01, *** =P<0.001 (Mann-Whitney test).

Assessing the effects of micro-stimulation via microelectrodes

The effects of DBS via microelectrodes were evaluated in the 6-OHDA lesioned rat model of PD using open field and limb use asymmetry test in a glass cylinder.

Open field test

The underlying hypothesis was that by selecting subgroups of implanted micro electrodes that produce beneficial effects and not using electrodes producing side effects, improved DBS would be accomplished. To evaluate this hypothesis we developed two statistical search strategies to find an appropriate combination of electrodes that are most effective in evoking displacement. **Strategy-I** (based on combining 8 electrodes in each test) and **Strategy-II** (based on combining 4 electrodes in each test). In addition, we evaluated possible synergistic effects on the stimulation threshold by using multiple electrodes to provide an idea of how many of the cluster electrodes need to be used.

Strategy-I, The stimulation current was fixed to 1.1 times the threshold current for evoking movements when using all microelectrodes. The mean threshold current/microelectrode was 20.2 ± 5.3 µA (mean ± SD). We tested 26 combinations each including eight electrodes during weeks 2, 4 and 6 (Fig. 2) and each combination was tested 3 times, therefore 78 trials per session. Different combinations of electrodes evoked different behavioral responses. Some combinations evoked fairly similar behavioral outcomes. Behaviors elicited ranged from increased locomotion, grooming and rearing, dyskinesia and increased rotations. Movement trajectories (forward movement), during stimulation, when using different sets of microelectrodes are shown in Fig. 5A, B.

Strategy-II, The stimulation current was kept at 1.1 times the threshold current found during the synergy test (see below) using four electrodes. 42 combinations each including four electrodes (week 6) were tested. The average threshold current/microelectrode was 36.6 ± 3.5 µA (mean ± SD), that is distinctly higher than when using 8 electrodes (see above). Stimulation with combinations of four electrodes evoked a similar plethora of behaviors as evoked when using a combination of eight electrodes (Fig. 5C, D). The four-electrodes which scored high in search **Strategy-I** varied to a certain degree from the best four electrodes found in the search **Strategy-II,** indicating that multiple combinations of electrodes can provide beneficial effects.

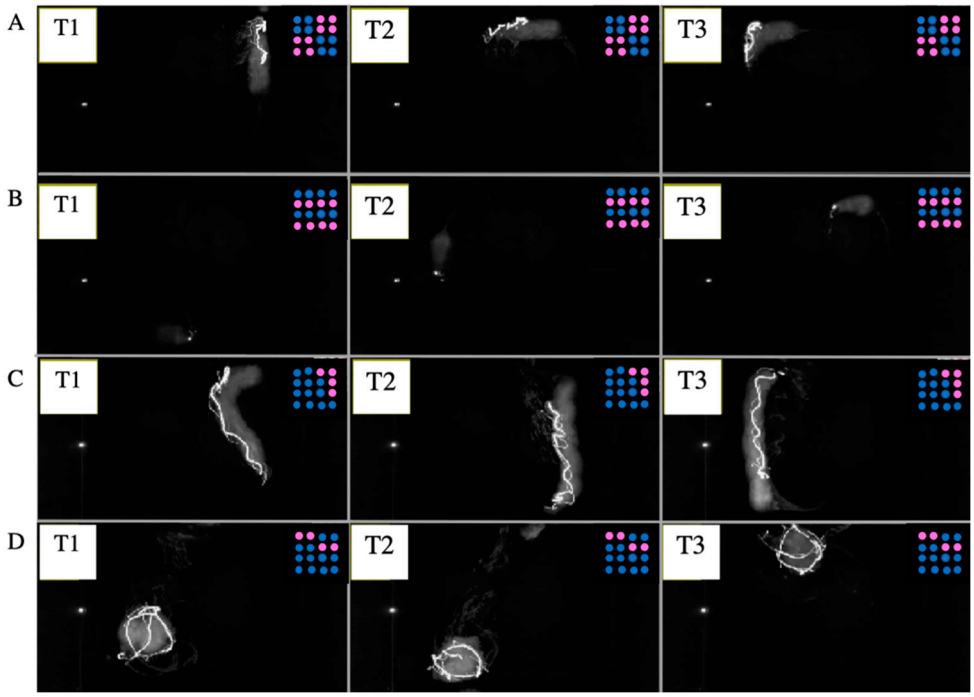

Fig. 5. Effects of different combinations of electrodes in the same rat. (A) Trajectory of movements during stimulation with combinations of eight electrodes consistently evoking forward displacement (T1,T2 and T3 represent trial 1, 2 and 3 in session 1. (B) Example of combination of eight electrodes,which evoked no movements in session 1. (C) Example of movement trajectory evoked using combination of four electrodes in session 4. (D) Example of rotational activity elicited using another combination of four electrodes in session 4. The electrode cluster is represented by the dots in the right corner of each panel. Active (stimulating) electrodes are represented by pink dots, while blue dots represent the inactive electrodes (not being used for stimulation). Reprinted (adapted) with permission from Paper-II.

Interestingly, very similar behavioral changes were evoked using the same set of electrodes in separate sessions of the experiments. For instance, the set of electrodes that evoked locomotor activity or rotation or no movement in one session, continued to evoke similar behavior in the following sessions. These results show that, by choosing an appropriate group of electrodes, a highly specific behavior can be elicited indicating that a high level of stimulation specificity can be achieved.

Synergy testing

We evaluated the synergistic effect, of using multiple electrode combinations, on the threshold of stimulating current (per electrode) for evoking motor changes when increasing the number of electrodes from 1 to 4. The four electrodes which got maximum displacement scores in the search **Strategy-I** were chosen for analyzing the synergistic effects of multiple electrodes. As can be seen in Fig. 6, the

threshold/electrode was significantly reduced when using more than one stimulating electrode. The threshold current when using four electrodes together was approximately 50% lower than the threshold current of a single electrode ($P<0.0001$).

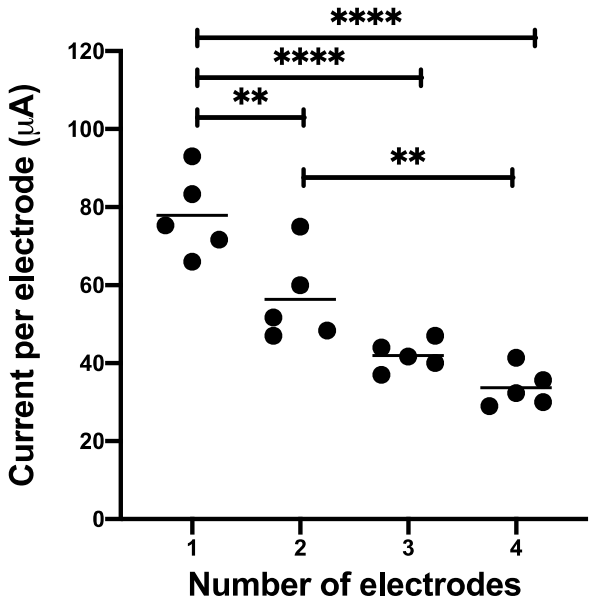

Fig. 6. Mean threshold current (horizontal line) and individual threshold values (black dots) when using 1-4 electrodes. When using multiple electrodes, the mean thershold current per electrode was significantly reduced as compared to using a single electrode (**P<0.01; ***P<0.001, ****P<0.0001). Reprinted (adapted) with permission from Paper-II.

Limb use asymmetry test/ Cylinder test

We then moved on to evaluate the effects of stimulation on the usage of the impaired forelimb, selecting microelectrodes on the basis of their beneficial effects on locomotion (using search **Strategy-I** and **-II**). During the baseline testing, when no stimulation was applied, the rats either exhibited no movement or mostly used the unimpaired forelimb (ipsilateral to lesion) while rising up and leaning against the glass wall. In three of five animals tested, a combination of the four electrodes which got the highest displacement scores using search **Strategy-I**, significantly improved the usage of the impaired forelimb, reaching close to equal usage. In the fourth animal, the stimulation current had to be increased in order to reach symmetry in the usage of the forelimb. The fifth animal, which only had a partial lesion of the

dopaminergic neurons exhibited symmetry in the usage of the paws already prior to stimulation and did not further improve during stimulation. By contrast, in the second cylinder test in which the four electrodes which showed the highest displacement scores in search **Strategy-II** were used, this often did not restore the forelimb asymmetry in the cylinder test. It thus appears that while many combinations of microelectrodes could produce beneficial effects on locomotion not all of them help restore motor control of the impaired forelimb.

Effect of the implanted electrode on surrounding tissue

We evaluated the effects of the implanted electrodes on surrounding neurons, glial activation and blood vessels appearances in Paper-II.

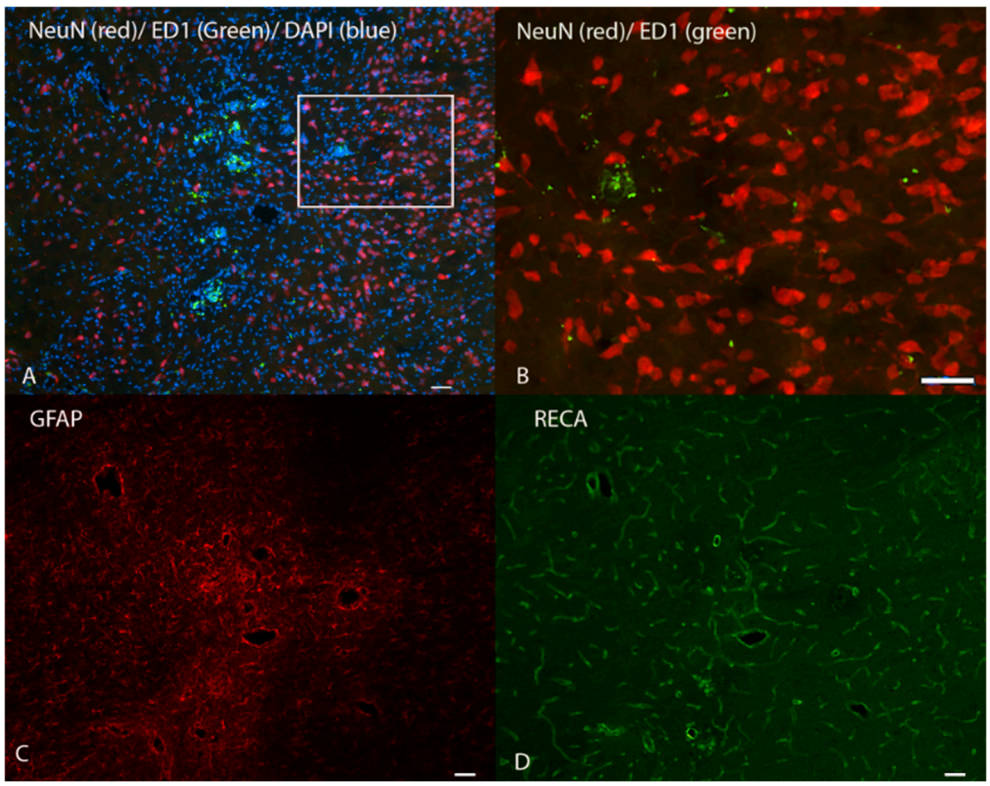

Fig. 7. Immunofluorescent staining of tissue reactions to an implanted microelectrode cluster. (A) NeuN (red), ED1 (green) and DAPI (blue). Rectangular box delineates the area magnified in B. (B) NeuN and ED1 staining near a single microelectrode in an area with high neuronal density. (C) GFAP and (D) RECA-staining of the same area 80 µm below the section in A . Scale bars= 50 µm. Reprinted (adapted) with permission from Paper-II.

Neuronal cell bodies were found in close vicinity (<10μm) of the individual microwires (Fig. 7A, B), at the depth corresponding to the stimulation site in all animals. Examination of GFAP staining revealed a diffuse astrocytic response around the single channels, with no apparent signs of condensed glial encapsulation (Fig. 7C). In addition, the response of the activated microglia was quantified around the single wires at electrophysiological relevant depth. Minute rings of activated microglia were observed around the voids left in the tissue after pulling out the microelectrodes. The average thickness of these rings was 8.9 ± 5.8 μm (Mean ±SD, Fig. 7B). Evaluation of RECA staining revealed no obvious changes in blood vessels density around the wires in the area of implantation (Fig. 7D).

Effects of hypothermia and ice-coat on the tissue response

To evaluate whether lowering the temperature of gelatinized probes to near 0°C has an effect on the tissue response, we compared the tissue response to implanted RT and cold (near 0°C) gelatinized needles. The tissue reactions were evaluated in cortex and striatum 1, and 7 days post stab with respect to neuronal density, neuronal void, microglial and astrocytic responses. No significant differences were observed between the two groups indicating that a mere reduction of temperature of the implant to ~0°C (from room temperature) does not affect neuronal survival or glial reactions.

To evaluate the effects on the tissue of adding a low friction ice-coat (thawing during insertion and therefore reaching near 0°C) around the gelatinised needles, the neuronal density, neuronal void as well as microglia activation and astrocyte response in the ice-coated needle group were compared to the cold needle group. The comparison was done in the cortical and striatal tissue at 1, and 7 days post stab in ROI 1, 2 and 3. Also, the neuronal densities in ROI 1, 2 and 3, were compared to their respective ROI 4. No substantial effects were seen on the glial reactions. Therefore, only the results on neurons are accounted for below.

One day post stab, the neuronal density in ROI 1 and 2 (i.e. within the track), in the ice-coated needle group was significantly higher than in the cold needle group (Fig. 8A, B) (ROI 1: 394% higher, $P < 0.05$; ROI 2: 116% higher, $P < 0.001$). When comparing, ROI 1, 2 and 3 to their respective ROI 4, there was a significant reduction in neuronal density for the cold needle group in ROI 1 (95%; $P < 0.0001$) and ROI 2 (69%; $P < 0.01$), but only in the ROI 1 (79%; $P < 0.01$) for the ice-coated group. In the striatum, a marked reduction in neuronal density in comparison to ROI

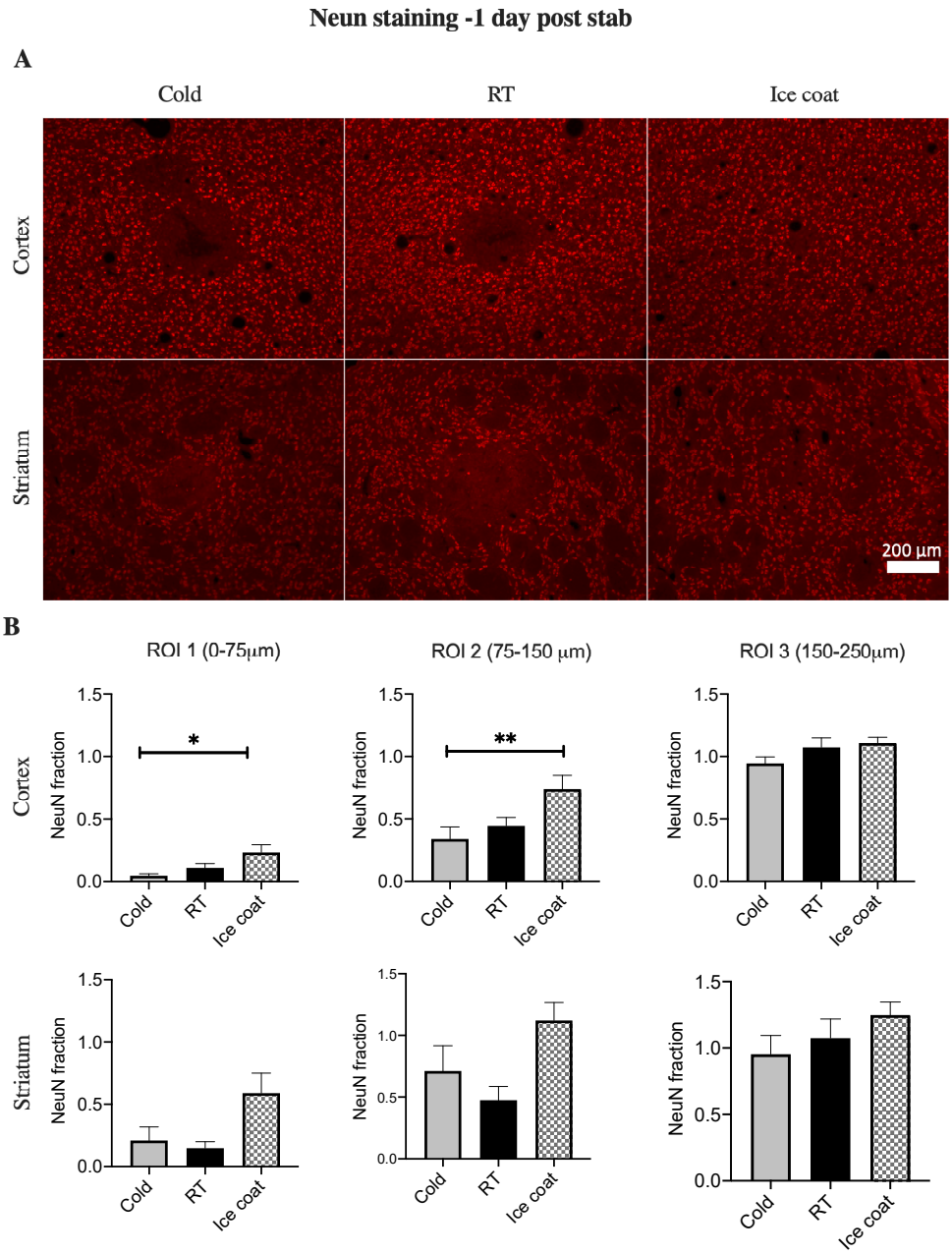

Fig. 8. Neuronal density 1 day after stab wound injury. (A) Representative immunohistological images of NeuN staining both in the cortex and the striatum one day post stab injury, comparing injuries due to cold gelatinized needles (~0°C), gelatinized needles at RT and gelatinized needles with a thawing ice-coat. (B) Neuronal density expressed as the ratio between the NeuN-stained area above the threshold and the total ROI area (In cortex; n = 10 for all groups. In striatum; n = 8 for cold and RT and n = 9 for ice-coated needles (Kruskal-Wallis Test, *P<0.05, **P<0.01). Reprinted (adapted) with permission from Paper-III.

4 was found in the cold needle group only, and this was also limited to ROI 1. By contrast, in the ice-coated needle group, there was no significant reduction in neuronal densities of ROI 1,2 and 3 when compared to ROI 4.

Seven days post stab, there was no significant difference between the neuronal densities of the ice-coated needle group when compared to the cold needle group in either cortex or striatum. When comparing ROI 1, 2 and 3 to ROI 4, the neuronal density in the cortex was significantly reduced in ROI 1 in both groups (67% for ice-coat, 87% for cold; $P < 0.05$). In the striatum, the neuronal density was, however, only reduced in the cold needle group, and confined to ROI 1 and 2 (52% and 40% respectively; $P < 0.01$).

One day post stab, the size of the neuronal void was significantly smaller in the cortex for the ice-coated needle group compared to the cold needle group ($P < 0.01$). There was no significant difference between the groups with respect to neuronal void at 7 days post stab, in cortex or striatum. These results together indicate that reducing the relative resistance between the implant and tissue by coating the probe with a super slippery ice-coat can mitigate the initial injury caused during implantation.

Effects of ice-coat on insertion force

After having found a major difference in tissue response when comparing ice-coated gelatinized needles with cold gelatinized needles, we further measured and compared the insertion forces exerted by these two groups during implantation.

As can be seen in Fig. 9, the insertion force when implanting an ice-coated needle was markedly reduced as compared to the insertion force when implanting a cold gelatinized needle. The mean insertion force during the initial part of the insertion (0-5 sec, penetration of meninges and brain) of ice-coated needles was 6.1 ± 2.3 mN which was 45% ($P < 0.01$) lower than the mean insertion force for cold gelatinized needles (11.1 ± 3.9 mN). The mean total force during the first 5 min of implantation (penetration + resting force phase) when using ice-coated needles was 3.2 ± 1.4 mN, which was 56% ($P < 0.01$) less than the mean total force for cold needles (7.2 ± 3.0 mN). The mean resting forces, at 8-10 min post-insertion, were similar and almost negligible (~0.4 mN, less than 5% of maximum) for both needle groups.

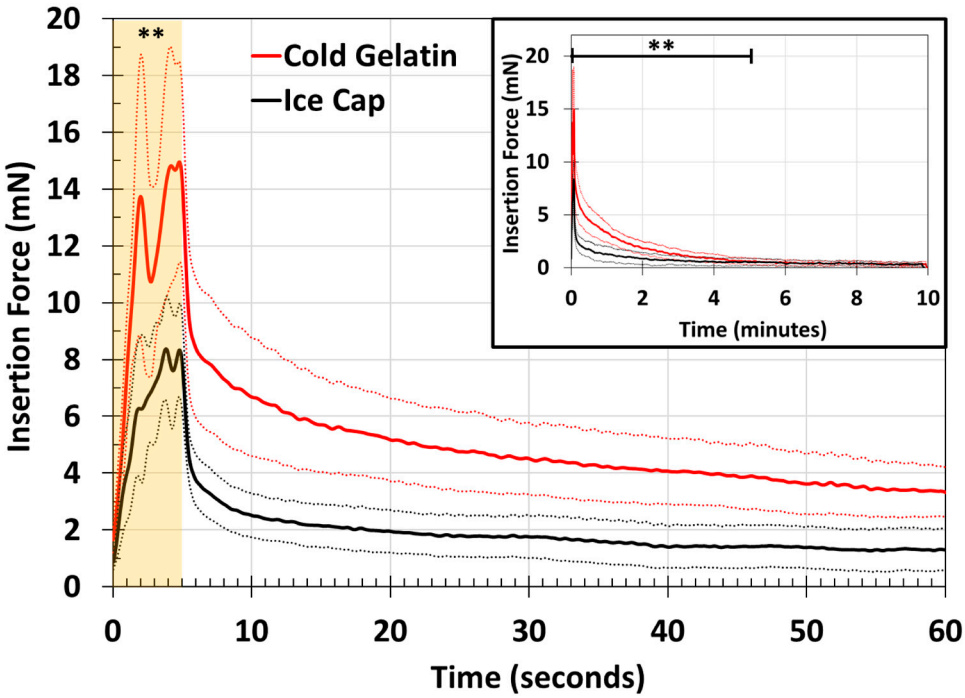

Fig. 9. Mean insertion force during insertion of cold gelatinised needles and Ice-coated gelatinized needles. Mean represented by solid lines and 95 % confidence interval (dotted lines) plots for ice-coated gelatinized needles (black, n = 8), and cold gelatinized needles (red, n = 8) inserted to a 5 mm depth at 1 mm/s speed, shown for t = 0–1 min and t = 0-10 min. Yellow shaded region denotes the 5 s penetration phase. (Student's t-test, $P<0.01$). Reprinted (adapted) with permission from Paper-III.

It can thus be concluded that the reduction in insertion force resulting from ice-coating is accompanied by beneficial effects on neuronal density.

Discussion and future perspectives

In the present thesis, novel microelectrode array designs and processes of manufacture, as well as implantation methods, were developed to mitigate injury and tissue reactions and to allow clusters of ultrathin microelectrodes to be implanted in deep brain targets to be used for stable neuronal recordings and highly specific stimulation in awake freely moving rodents.

Novel implantation technique for improving biocompatibility

Implantable neuroelectronic interfaces have contributed significantly to our general understanding of brain physiology during normal and pathological conditions. However, their very insertion inflicts mechanical injury which leads to an immune response. This changes the normal physiochemical milieu of the tissue [41]. Acute changes in the neuronal environment includes tissue strain, blood-brain barrier rupture, signaling blockade, and loss of perfusion and formation of a microglia/ astrocytic capsule around the implant [41]. As a consequence, a reduction of the acute injury is of key importance. For this reason, many previous studies have analyzed parameters such as insertion speed and tissue resistance [47, 85].

Previous studies have shown that thin and flexible microelectrodes are more biocompatible [17, 60, 61]. However, they are prone to mechanical buckling and consequent deviation from the intended track during implantation. Therefore, various methods have been developed to implant flexible microelectrodes. For example, methods adhering flexible electrodes to a stiff guide during implantation and removal of the stiff guide once electrodes are in place [86], or passing microwires through a guide tube [87], have been used. However, the insertion of a stiff guide or guide tube causes tissue damage due to their bigger size (than the electrodes). In addition, their subsequent removal from the tissue may displace the implanted microelectrodes. Other methods that have been used to implant flexible electrodes is coating them with sugar [88], or PEG [89]. One problem with these types of coating is that, the glue dissolves fast when in contact with body fluids,

making it difficult to implant in deep brain tissue and reach the intended target depth with accuracy. Given that the highest insertion resistance during implantation occurs at the meninges, topical application of collagenase enzyme has been tried to open them and reduce the resistance [90]. However, these latter implantation techniques still depend on sufficient inherent stiffness of the electrode. It should also be noted that most flexible microelectrodes have been developed for cortical recordings. The problem of instability during insertion of flexible electrodes is much bigger when implanting in deeper targets.

In this thesis, we were, for the first time able to implant ultrathin microelectrodes in deep target structures, without the support of stiff guides or cannulas, by embedding them in dry gelatin. Gelatin is known to be highly biocompatible, non-allergenic, and after implantation in the brain, it is degraded to amino acids by resident matrix metalloproteinases (MMP-2 and MMP-9) [62]. Previous studies in our laboratory have also shown that gelatin significantly decreases microglial reactions, enhances neuronal survival, and helps in faster reparation of the blood-brain barrier near the implantation site [17, 62, 64].The gelatin material is thus not only a vehicle but also significantly contributes to an improved situation in the tissue after implantation. The finding in this thesis of relatively high amplitude neuronal signals (Paper-I), low stimulation thresholds (Paper-II), neurons in close vicinity (<10 μm), and minimal microglial and astrocytic responses (Paper-II), confirms a high biocompatibility of the gelatin. However, the mechanisms behind the beneficial effects of gelatin are still not entirely clear. One possibility is that gelatin provides a relatively low friction outer layer when hydrated and that low friction during insertion reduce damage to the neuronal tissue. This “mechanical injury” theory is in line with the idea that neurons are exquisitely susceptible to microforces [59]. To further analyze the role of friction, we developed a super slippery coating on the gelatin vehicle, i.e. the addition of an ice-coat. Indeed, the reduction of insertion forces, despite a larger diameter of the probe, was accompanied by a significant reduction of the acute loss of neurons and notably minute residual forces 8-10 minutes after insertion. These result thus supports the idea that friction (tearing forces) during insertion is of importance (Paper-III). Conceivably, the nanofiber web of the meninges and extracellular matrix cannot cling to melting ice during the insertion. Since there was no difference between the RT probes and the frozen probes (held at 0^{o}C during insertion), the effect of the ice-coat was not due to low temperature. That frozen probes did not do any harm also opens up interesting future possibilities.

Deep Brain Recording

Neuroelectronic interfaces, which can be used to record neuronal signals and stimulate for long time with spatial precision, are of high importance not only for functional understanding of complex neural circuitry but also for therapeutic neuromodulation. However, the performance of implanted neuroelectronic devices has been quite variable in the past and often show progressive deterioration over time (few weeks, months or years) after implantation [91]. The progressive deterioration of recording capacity of implanted devices is assumed to be due to progressive tissue reactions driven by microforces between the tissue and the implant [35, 40, 92]. Flexible microelectrodes, which can better follow micromotions of the brain may therefore mitigate the problem [17, 93]. Thus to improve mechanical compliance between the implant and tissue, flexible polymer (such as polyamide and parylene) based neuroelectronic devices have been developed [32, 94, 95]. However, the majority of these types of devices are designed for cortical recording [96]. Hence, much of what is currently known on neuronal signaling in deep structures in awake freely moving animals is still based on recordings using stiff electrodes that induce considerable tissue reactions. To enable implantation of ultra-flexible microelectrodes into deep targets we made use of needle shaped gelatin vehicles allowing multiple electrodes to be inserted through a narrow track-line to pre-target levels and then made to spread out in the target area. During the entire period of eight weeks after implantation, the overall impedance and SNR remained stable. In view of that the impedance of implanted electrodes is known to be affected by the tissue reactions [97], normally increasing during the first weeks, in parallel with an increasing gliosis [98, 99], the stable impedance we found indicates a more stable, i.e. non-increasing, gliosis around ultra-flexible microelectrodes. In addition, the stable SNR found in Paper-I, indicates preservation of viable neurons near recording sites which was confirmed in the subsequent histological examination in Paper-II. Notably, the quality of the recordings did not decline significantly during the eight week observation time, which is in sharp contrast to previous studies [100, 101].

Deep Brain Stimulation

Implanted electrodes for electrical stimulation of neurons have been widely used both in the clinic and research. Currently used clinical DBS electrodes, for treatment of e.g. Parkinson disease, are rather large often in the millimetre scale, as compared to microelectrodes used in research. Consequently, the tissue reactions and loss of

neurons are typically in the millimetre scale [102] precluding precise stimulation of smaller groups of neurons. Due to the relatively large surface area of their stimulation site, current can be ejected that effectively stimulate neuronal tissue beyond the scarring. However, the profuse spread of the current necessary to produce beneficial effects, in turn hinder a detailed analysis of the underlying neuronal mechanisms of the beneficial effects. Consequently, the mechanisms behind DBS are still poorly understood [103]. Moreover, adverse effects, caused by current spread to unintended brain areas, are often difficult to avoid [78]. Hence, while DBS of the subthalamic nucleus (STN) can be highly effective in treating the motor symptoms of PD patients, it has been associated with worsening of speech and cognitive symptoms [104, 105]. To mitigate these problems, the latest DBS electrode design ("Cartesia" from Boston Scientific, "Model 6180" from Abbott) for clinical use is equipped with multiple segmented stimulation sites along the circumference of the probe [39], allowing steering of stimulating current in a pre-defined horizontal plane [106]. This novel design partially solves the problem of how to avoid side effects [107]. However, since stimulation sites are placed on the same physical body, differential stimulation of functionally distinct territories within the same nuclei is far from optimal (Fig. 10A).

Microelectrodes can only stimulate neurons locally (Fig. 10B) due to their smaller surface area when adhering to established safety levels (30 μC/cm2), [108, 109], and therefore need to be precisely positioned in the tissue. However, it is presently not clear whether the stimulation should be made within or outside the STN (for example in zona incerta) to produce optimal beneficial effects [110-112]. Given that, the exact brain sites to be stimulated are not yet well defined, it becomes challenging to locate the right spot to microstimulate for achieving therapeutically beneficial effects. One of the main aims of this thesis was therefore to evaluate if micro-stimulation, based on a cluster of microelectrodes spread out in a target area, is a viable option for brain stimulation in the clinic. To overcome the problems of limited stimulation range of microelectrodes, a cluster of ultra-flexible (and therefore biocompatible) microelectrodes was developed and evaluated (Paper-II). The hypothesis was that by selection of appropriate subsets of microelectrodes, that produce beneficial effects upon stimulation, an increased stimulation specificity and a reduction of side effects can be achieved.

This hypothesis was confirmed in a rat model of PD. Importantly, stimulation thresholds for therapeutic effects were well below safety levels. Although promising, it remains to be evaluated if ultra-flexible microelectrodes will be able to deliver sufficient stimulation current in animals/humans with a bigger brain size.

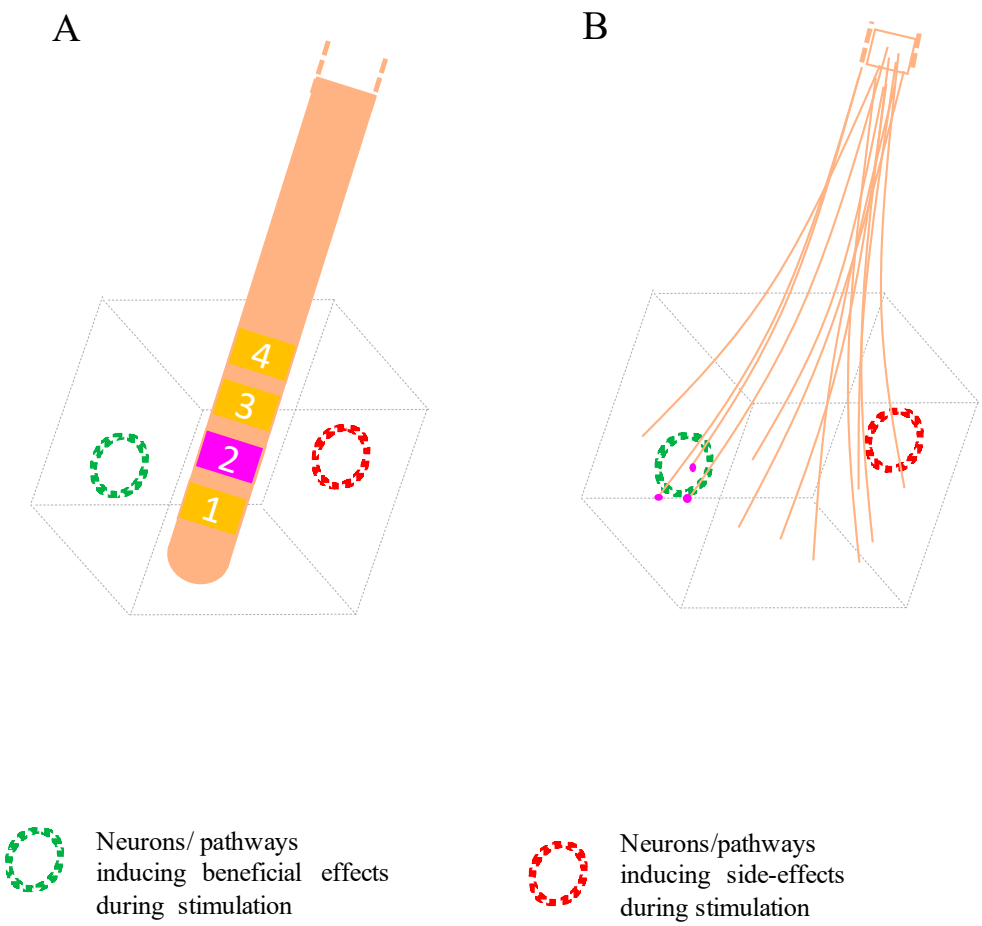

Fig. 10.Schematic comparision of the stimulation field produced by a conventional DBS electrode and the developed multichannel cluster electrode. (A) Conventional DBS electrode with four stimulation sites. (B) DBS electrode developed in this thesis with multiple stimulating microelectrodes. Violet color indicates the active channel/sites and yellow color indicates the spread of stimulation current. Green colored circle represents the neurons/pathways, which evoke the good therapeutic effects upon stimulating. Red colored circles represents neurons/ pathways which evoke side effects upon stimulation.

The fact that the threshold current for therapeutic effects was much lower when using multiple microelectrodes compared to using a single microelectrode suggest that the problem of limited current delivery can be overcome by using many microelectrodes in larger brains. However, an increased number of microelectrodes, will, of course, also increase the time consumption to find the most effective electrodes, given the increased number of possible microelectrode combinations. For example, there are 12870 possible combinations of 8 electrodes that can be

selected from a group of 16 electrodes. We, therefore developed a novel statistical method to reduce the number of tests necessary to find useful combinations of the microelectrodes. Interestingly, the statistical scanning method introduced in Paper-II, required only a small number of trials to find beneficial combinations, indicating that many combinations, not just one can be of therapeutic use.

One current trend in brain stimulation is to develop “closed-loop” stimulation, using conventional electrodes, wherein stimulation is dependent on the information extracted from recorded neuronal activity [113]. This way stimulation can be turned on and off depending on the need. The cluster design of the developed microelectrode probe, providing an increased specificity and reduced side effects, can be tailored to allow closed-loop DBS, wherein a subset of microelectrodes is used for detecting neural activity, and another subset for stimulation. Such electrode constructs may, in combination with appropriate software, provide the basis for dynamical fine tuning of brain stimulation, thereby optimizing stimulation therapy in the future.

Acknowledgements

I would like to express my gratitude to all of you who had contributed to this thesis work and along the path left treasured memories.

My immeasurable appreciation and deepest gratitude to my principal supervisor *Jens Schouenborg*. You are an inspiration and of course amazing mentor with endless patience and kindness. Even in your busiest days, you always have time to listen to my crazy ideas and answer my queries meticulously with pleasure. I admire your astonishing determination towards your visions and your ability to remember the minutest details of every project. Your word "Mohsin! Devil lies in details" got stuck in my brain. Perhaps the most important thing which you taught me is going into detail and believing in your own ideas. You have always shown trust and given me the freedom for trying new ideas. During the years, I learned a lot from you not only about research but life in general. On many occasions, you have advised me on matters outside work, which helped me in making the right decisions. When family issues overlapped with the work, you have been always supportive. Discussions with you on various topics and your untiring feedbacks has profoundly influenced my thinking. Thanks a million for strengthening me with your continuous support, motivation and patience.

Angela Cenci-Nilsson, I started the journey of my PhD in your lab. You provided me the opportunity to come from the other side of the world and work in your group. Your doors were always open for discussions and invaluable feedback. Your amazing passion for Parkinson's disease research is extremely contagious. You are the first stepping stone in my professional development. Thanks a lot for all your trust and unreserved support.

Per Petersson, you are a unique blend of affable and kind-hearted personality, always ready to help with enthusiasm. I remember our first meeting when I came for an interview, you were so friendly and kind as usual. Thank you very much for all your kind helps and support.

Marcus Granmo, Thank you.

Martin Garwicz and *Nils Danielsen*, Thank you for your guidance and support.

Lina. P. and *Jonas*, my wonderful teachers and partners of everyday activities. Your help and guidance are highly appreciated.

Lina P, you are my trusted and critical reviewer. I appreciate the painstaking efforts to review my manuscripts. I should admit that I didn't use to like your critical comments and questions initially ☺ but they were quite helpful at the end. Thank you Lina for your help and making work fun.

Jonas, you were always there, bearing all my frustration, supporting and cheering me up when I was having a hard time. I was telling you my "life coach" Joking, but seriously you have surpassed it, fulfilled the responsibility of elder brother. Thanks a lot, bro!!!!

Palmi, the genius of all analysis and programming. It is amazing to see how thorough you are with your work. Without your kind help in analysis and programming, these studies would not have been possible. Thank you for being an amazing friend and colleague.

Matilda, our lab's world traveler! Always cheering and smiling. Your roti making skills are highly impressive, I cannot even make such good roti being an Indian. Remember the border between Indian and Italian territory ☺. Thank you for bringing all the fun.

Michael! my friend and coffee partner. I am impressed by your caring attitude and handy skills of making new things from scratch. It was such a pleasure to meet your cute family. Thanks for the good times and your company buddy!

Alex, my cool friend! We began as co-workers many years ago and ended up becoming friends immediately. Always ready to help. Thank you for all your kind help and ….. you know it ☺.

Linda, you have an exceptional quality of management and a positive attitude. Thank you for solving everyday challenges and coffee mug ☺.

Agneta, Master of protocols and histological techniques. Thank you for your kind help in the histology lab.

Lina G, My new office mate, thank you for good talks and fika

Nedjeljka Ivice, Finally I can write, the right spelling of your name Nela! It was fun to work with you.

Johan, the writer! It is always fun to talk with you.

Ale, The Philosopher! You have a unique way of looking at things.

Niklas and *Lucas*, thank you for being good colleagues.

Robin and *Daniel*, thank you for the good talks.

Jorgen, smart and energetic guy! Thank you.

Vlora and *Martin*, my first friends and family in Sweden. I feel blessed to have friends like you. Thank you for being there for us.

Lovisa and *Paar*, you are no less than family. We had amazing times together. Thank you!

I would like to thank my colloquies and friends from BMC: *Daniella*, *Elisbet*, *Tim*, *Very*, *Hanna*, *Irene*, *Francesco*, *Zisis* and *Gurdal*.

I wish to thank Kämnärgsvägen PhD student folk: *Karthiken*, *Sandy*, *Chinmay*, Idris, *Aftab*, *Deepti* and *Kavita*. A special thanks to *Srikanth* and *Rama* for all your support and help.

Tanja and *Fakir*, lucky to have friends like you. Thank you for your constant support and encouragement and babysitting.

Aleem, *Fatima, Matiullah and Arshi*, thank you for fun times.

Last but not least, my family. I want to thank my mother and father, for the countless favors and for making me into the person who I am today. My brothers and sisters, you have been my strength. Special thanks to *Mahmood bhaiyya, Mujeeb bhaiyya* and *Mujahid bhaiyya* for taking care of me, educating me, strengthening me, encouraging me. I am thankful to "Almighty Allah" for blessing brothers like you. *Moin*, mere choto, I still call Hamza sometime with your name. *Munni baji*, *Maryam* and *Sabbu*, my sister thank you for unconditional love. *Farhana bhabi* and *Nazia bhabi*, thank you for your motherly compassion, I still miss the delicious food made by you people.

My kids, *Konain* , *Hamza* and *Nashrah*. You people filled my life with joy. You people mean a whole world to me.

To *Juveria*, my wife, my best friend, and my dependable companion. We have overcome many life's challenges together. What would I do without you? I want to thank "Almighty Allah" for blessing you as my wife. I want to thank you for your care, your compassion, your love and for being an incredible mother to our kids.

References

1. Hodgkin, A.L. and A.F. Huxley, *A quantitative description of membrane current and its application to conduction and excitation in nerve.* J Physiol, 1952. **117**(4): p. 500-44.
2. Marzullo, T.C., *The Missing Manuscript of Dr. Jose Delgado's Radio Controlled Bulls.* J Undergrad Neurosci Educ, 2017. **15**(2): p. R29-R35.
3. Marg, E. and J.E. Adams, *Indwelling multiple micro-electrodes in the brain.* Electroencephalogr Clin Neurophysiol, 1967. **23**(3): p. 277-80.
4. Kipke, D.R., W. Shain, G. Buzsaki, E. Fetz, J.M. Henderson, J.F. Hetke, and G. Schalk, *Advanced neurotechnologies for chronic neural interfaces: new horizons and clinical opportunities.* J Neurosci, 2008. **28**(46): p. 11830-8.
5. Leuthardt, E.C., G. Schalk, J. Roland, A. Rouse, and D.W. Moran, *Evolution of brain-computer interfaces: going beyond classic motor physiology.* Neurosurgical Focus, 2009. **27**(1).
6. Kennedy, P.R. and R.A. Bakay, *Restoration of neural output from a paralyzed patient by a direct brain connection.* Neuroreport, 1998. **9**(8): p. 1707-11.
7. Kalinowsky, L.B., *History of convulsive therapy.* Ann N Y Acad Sci, 1986. **462**: p. 1-4.
8. Gol, A., *Relief of pain by electrical stimulation of the septal area.* J Neurol Sci, 1967. **5**(1): p. 115-20.
9. Heath, R., W. Mickle, E. Ramey, and D. O'Doherty, *Electrical studies on the unanesthetized brain.* 1960.
10. Benabid, A.L., P. Pollak, C. Gervason, D. Hoffmann, D.M. Gao, M. Hommel, J.E. Perret, and J. de Rougemont, *Long-term suppression of tremor by chronic stimulation of the ventral intermediate thalamic nucleus.* Lancet, 1991. **337**(8738): p. 403-6.
11. Pollak, P., A.L. Benabid, C. Gross, D.M. Gao, A. Laurent, A. Benazzouz, D. Hoffmann, M. Gentil, and J. Perret, *[Effects of the stimulation of the subthalamic nucleus in Parkinson disease].* Rev Neurol (Paris), 1993. **149**(3): p. 175-6.
12. Sironi, V.A., *Origin and evolution of deep brain stimulation.* Front Integr Neurosci, 2011. **5**: p. 42.
13. Gardner, J., *A history of deep brain stimulation: Technological innovation and the role of clinical assessment tools.* Social Studies of Science, 2013. **43**(5): p. 707-728.

14. Szostak, K.M., L. Grand, and T.G. Constandinou, *Neural Interfaces for Intracortical Recording: Requirements, Fabrication Methods, and Characteristics.* Frontiers in Neuroscience, 2017. **11**.
15. Hong, G. and C.M. Lieber, *Novel electrode technologies for neural recordings.* Nat Rev Neurosci, 2019. **20**(6): p. 330-345.
16. Rheinberger, M.B. and H.H. Jasper, *Electrical Activity of the Cerebral Cortex in the Unanesthetized Cat.* American Journal of Physiology, 1937. **119**(1): p. 186-196.
17. Lind, G., C.E. Linsmeier, J. Thelin, and J. Schouenborg, *Gelatine-embedded electrodes-a novel biocompatible vehicle allowing implantation of highly flexible microelectrodes.* Journal of Neural Engineering, 2010. **7**(4).
18. Agorelius, J., F. Tsanakalis, A. Friberg, P.T. Thorbergsson, L.M.E. Pettersson, and J. Schouenborg, *An array of highly flexible electrodes with a tailored configuration locked by gelatin during implantation-initial evaluation in cortex cerebri of awake rats.* Frontiers in Neuroscience, 2015. **9**.
19. Nicolelis, M.A.L., *Methods for neural ensemble recordings*. 2nd ed. Frontiers in neuroscience. 2008, Boca Raton: CRC Press. xx, 269 p.
20. Merlo, M.W., R.L. Snyder, J.C. Middlebrooks, and M. Bachman, *Microelectrode arrays fabricated using a novel hybrid microfabrication method.* Biomedical Microdevices, 2012. **14**(1): p. 193-205.
21. Kaltenbach, J.A. and G.L. Gerstein, *A Rapid Method for Production of Sharp Tips on Preinsulated Microwires.* Journal of Neuroscience Methods, 1986. **16**(4): p. 283-288.
22. Cirelli, R.A., G.P. Watson, and O. Nalamasu, *Optical Lithography* in *Encyclopedia of Materials: Science and Technology*, K.H.J. Buschow, Editor. 2001, Elsevier p. 6441-6448.
23. Hassler, C., T. Boretius, and T. Stieglitz, *Polymers for Neural Implants (vol 49, pg 18, 2011).* Journal of Polymer Science Part B-Polymer Physics, 2011. **49**(3): p. 255-255.
24. Gwon, T.M., C. Kim, S. Shin, J.H. Park, J.H. Kim, and S.J. Kim, *Liquid Crystal Polymer (LCP)-based Neural Prosthetic Devices.* Biomedical Engineering Letters, 2016. **6**(3): p. 148-163.
25. Lin, C.H., G.B. Lee, B.W. Chang, and G.L. Chang, *A new fabrication process for ultra-thick microfluidic microstructures utilizing SU-8 photoresist.* Journal of Micromechanics and Microengineering, 2002. **12**(5): p. 590-597.
26. Suner, S., M.R. Fellows, C. Vargas-Irwin, G.K. Nakata, and J.P. Donoghue, *Reliability of signals from a chronically implanted, silicon-based electrode array in non-human primate primary motor cortex.* IEEE Trans Neural Syst Rehabil Eng, 2005. **13**(4): p. 524-41.
27. Vetter, R.J., J.C. Williams, J.F. Hetke, E.A. Nunamaker, and D.R. Kipke, *Chronic neural recording using silicon-substrate microelectrode arrays implanted in cerebral cortex.* Ieee Transactions on Biomedical Engineering, 2004. **51**(6): p. 896-904.

28. Rousche, P.J. and R.A. Normann, *Chronic recording capability of the Utah Intracortical Electrode Array in cat sensory cortex.* Journal of Neuroscience Methods, 1998. **82**(1): p. 1-15.
29. Kipke, D.R., R.J. Vetter, J.C. Williams, and J.F. Hetke, *Silicon-substrate intracortical microelectrode arrays for long-term recording of neuronal spike activity in cerebral cortex.* Ieee Transactions on Neural Systems and Rehabilitation Engineering, 2003. **11**(2): p. 151-155.
30. Nguyen, J.K., D.J. Park, J.L. Skousen, A.E. Hess-Dunning, D.J. Tyler, S.J. Rowan, C. Weder, and J.R. Capadona, *Mechanically-compliant intracortical implants reduce the neuroinflammatory response.* Journal of Neural Engineering, 2014. **11**(5).
31. Lee, K., A. Singh, J.P. He, S. Massia, B. Kim, and G. Raupp, *Polyimide based neural implants with stiffness improvement.* Sensors and Actuators B-Chemical, 2004. **102**(1): p. 67-72.
32. Ejserholm, F., P. Kohler, M. Granmo, J. Schouenborg, M. Bengtsson, and L. Wallman, *mu-Foil Polymer Electrode Array for Intracortical Neural Recordings.* IEEE J Transl Eng Health Med, 2014. **2**: p. 1500207.
33. Xiang, Z.L., S.C. Yen, N. Xue, T. Sun, W.M. Tsang, S.S. Zhang, L.D. Liao, N.V. Thakor, and C. Lee, *Ultra-thin flexible polyimide neural probe embedded in a dissolvable maltose-coated microneedle.* Journal of Micromechanics and Microengineering, 2014. **24**(6).
34. Kim, B.J., J.T.W. Kuo, S.A. Hara, C.D. Lee, L. Yu, C.A. Gutierrez, T.Q. Hoang, V. Pikov, and E. Meng, *3D Parylene sheath neural probe for chronic recordings.* Journal of Neural Engineering, 2013. **10**(4).
35. Gilletti, A. and J. Muthuswamy, *Brain micromotion around implants in the rodent somatosensory cortex.* Journal of Neural Engineering, 2006. **3**(3): p. 189-195.
36. Biran, R., D.C. Martin, and P.A. Tresco, *The brain tissue response to implanted silicon microelectrode arrays is increased when the device is tethered to the skull.* Journal of Biomedical Materials Research Part A, 2007. **82a**(1): p. 169-178.
37. Butson, C.R. and C.C. McIntyre, *Role of electrode design on the volume of tissue activated during deep brain stimulation.* Journal of Neural Engineering, 2006. **3**(1): p. 1-8.
38. Hariz, M., *Deep brain stimulation: new techniques.* Parkinsonism Relat Disord, 2014. **20 Suppl 1**: p. S192-6.
39. Anderson, D.N., B. Osting, J. Vorwerk, A.D. Dorval, and C.R. Butson, *Optimized programming algorithm for cylindrical and directional deep brain stimulation electrodes.* Journal of Neural Engineering, 2018. **15**(2).
40. Prodanov, D. and J. Delbeke, *Mechanical and Biological Interactions of Implants with the Brain and Their Impact on Implant Design.* Frontiers in Neuroscience, 2016. **10**.
41. Kozai, T.D., A.S. Jaquins-Gerstl, A.L. Vazquez, A.C. Michael, and X.T. Cui, *Brain tissue responses to neural implants impact signal sensitivity and intervention strategies.* ACS Chem Neurosci, 2015. **6**(1): p. 48-67.

42. Pulsinelli, W.A., J.B. Brierley, and F. Plum, *Temporal Profile of Neuronal Damage in a Model of Transient Forebrain Ischemia.* Annals of Neurology, 1982. **11**(5): p. 491-498.
43. Pulsinelli, W.A. and T.E. Duffy, *Regional Energy-Balance in Rat-Brain after Transient Forebrain Ischemia.* Journal of Neurochemistry, 1983. **40**(5): p. 1500-1503.
44. Davalos, A., J. Castillo, J. Marrugat, J.M. Fernandez-Real, A. Armengou, P. Cacabelos, and R. Rama, *Body iron stores and early neurologic deterioration in acute cerebral infarction.* Neurology, 2000. **54**(8): p. 1568-1574.
45. Gu, Y., C.M. Dee, and J. Shen, *Interaction of free radicals, matrix metalloproteinases and caveolin-1 impacts blood-brain barrier permeability.* Front Biosci (Schol Ed), 2011. **3**: p. 1216-31.
46. Abdul-Muneer, P.M., N. Chandra, and J. Haorah, *Interactions of Oxidative Stress and Neurovascular Inflammation in the Pathogenesis of Traumatic Brain Injury.* Molecular Neurobiology, 2015. **51**(3): p. 966-979.
47. Welkenhuysen, M., A. Andrei, L. Ameye, W. Eberle, and B. Nuttin, *Effect of Insertion Speed on Tissue Response and Insertion Mechanics of a Chronically Implanted Silicon-Based Neural Probe.* Ieee Transactions on Biomedical Engineering, 2011. **58**(11): p. 3250-3259.
48. Casanova, F., P.R. Carney, and M. Sarntinoranont, *In vivo evaluation of needle force and friction stress during insertion at varying insertion speed into the brain.* Journal of Neuroscience Methods, 2014. **237**: p. 79-89.
49. Kozai, T.D.Y., A.L. Vazquez, C. LWeaver, S.G. Kim, and X.T. Cui, *In vivo two-photon microscopy reveals immediate microglial reaction to implantation of microelectrode through extension of processes.* Journal of Neural Engineering, 2012. **9**(6).
50. Stence, N., M. Waite, and M.E. Dailey, *Dynamics of microglial activation: A confocal time-lapse analysis in hippocampal slices.* Glia, 2001. **33**(3): p. 256-266.
51. Raivich, G., M. Bohatschek, C.U.A. Kloss, A. Werner, L.L. Jones, and G.W. Kreutzberg, *Neuroglial activation repertoire in the injured brain: graded response, molecular mechanisms and cues to physiological function.* Brain Research Reviews, 1999. **30**(1): p. 77-105.
52. Salatino, J.W., K.A. Ludwig, T.D.Y. Kozai, and E.K. Purcell, *Glial responses to implanted electrodes in the brain.* Nature Biomedical Engineering, 2017. **1**(11): p. 862-877.
53. Smith, J.A., A. Das, S.K. Ray, and N.L. Banik, *Role of pro-inflammatory cytokines released from microglia in neurodegenerative diseases.* Brain Research Bulletin, 2012. **87**(1): p. 10-20.
54. Barrese, J.C., N. Rao, K. Paroo, C. Triebwasser, C. Vargas-Irwin, L. Franquemont, and J.P. Donoghue, *Failure mode analysis of silicon-based intracortical microelectrode arrays in non-human primates.* Journal of Neural Engineering, 2013. **10**(6).

55. Szarowski, D.H., M.D. Andersen, S. Retterer, A.J. Spence, M. Isaacson, H.G. Craighead, J.N. Turner, and W. Shain, *Brain responses to micro-machined silicon devices.* Brain Research, 2003. **983**(1-2): p. 23-35.
56. Roitbak, T. and E. Sykova, *Diffusion barriers evoked in the rat cortex by reactive astrogliosis.* Glia, 1999. **28**(1): p. 40-48.
57. Lempka, S.F., S. Miocinovic, M.D. Johnson, J.L. Vitek, and C.C. McIntyre, *In vivo impedance spectroscopy of deep brain stimulation electrodes.* Journal of Neural Engineering, 2009. **6**(4).
58. Nolta, N.F., M.B. Christensen, P.D. Crane, J.L. Skousen, and P.A. Tresco, *BBB leakage, astrogliosis, and tissue loss correlate with silicon microelectrode array recording performance.* Biomaterials, 2015. **53**: p. 753-762.
59. Lind, G., C.E. Linsmeier, and J. Schouenborg, *The density difference between tissue and neural probes is a key factor for glial scarring.* Scientific Reports, 2013. **3**.
60. Gallentoft, L., L.M.E. Pettersson, N. Danielsen, J. Schouenborg, C.N. Prinz, and C.E. Linsmeier, *Size-dependent long-term tissue response to biostable nanowires in the brain.* Biomaterials, 2015. **42**: p. 172-183.
61. Kozai, T.D.Y., N.B. Langhals, P.R. Patel, X.P. Deng, H.N. Zhang, K.L. Smith, J. Lahann, N.A. Kotov, and D.R. Kipke, *Ultrasmall implantable composite microelectrodes with bioactive surfaces for chronic neural interfaces.* Nature Materials, 2012. **11**(12): p. 1065-1073.
62. Kumosa, L.S., V. Zetterberg, and J. Schouenborg, *Gelatin promotes rapid restoration of the blood brain barrier after acute brain injury.* Acta Biomaterialia, 2018. **65**: p. 137-149.
63. Lee, H.C., F. Ejserholm, J. Gaire, S. Currlin, J. Schouenborg, L. Wallman, M. Bengtsson, K. Park, and K.J. Otto, *Histological evaluation of flexible neural implants; flexibility limit for reducing the tissue response?* Journal of Neural Engineering, 2017. **14**(3).
64. Kohler, P., A. Wolff, F. Ejserholm, L. Wallman, J. Schouenborg, and C.E. Linsmeier, *Influence of Probe Flexibility and Gelatin Embedding on Neuronal Density and Glial Responses to Brain Implants.* Plos One, 2015. **10**(3).
65. Berardelli, A., J.C. Rothwell, P.D. Thompson, and M. Hallett, *Pathophysiology of bradykinesia in Parkinson's disease.* Brain, 2001. **124**(Pt 11): p. 2131-46.
66. Jankovic, J., *Parkinson's disease: clinical features and diagnosis.* J Neurol Neurosurg Psychiatry, 2008. **79**(4): p. 368-76.
67. Mhyre, T.R., J.T. Boyd, R.W. Hamill, and K.A. Maguire-Zeiss, *Parkinson's disease.* Subcell Biochem, 2012. **65**: p. 389-455.
68. Snider, S.R., S. Fahn, W.P. Isgreen, and L.J. Cote, *Primary sensory symptoms in parkinsonism.* Neurology, 1976. **26**(5): p. 423-9.
69. Fahn, S. and G. Parkinson Study, *Does levodopa slow or hasten the rate of progression of Parkinson's disease?* J Neurol, 2005. **252 Suppl 4**: p. IV37-IV42.

70. Pantcheva, P., S. Reyes, J. Hoover, S. Kaelber, and C.V. Borlongan, *Treating non-motor symptoms of Parkinson's disease with transplantation of stem cells.* Expert Rev Neurother, 2015. **15**(10): p. 1231-40.
71. Lozano, A.M., A.E. Lang, W.D. Hutchison, and J.O. Dostrovsky, *New developments in understanding the etiology of Parkinson's disease and in its treatment.* Curr Opin Neurobiol, 1998. **8**(6): p. 783-90.
72. Bjornestad, A., E.B. Forsaa, K.F. Pedersen, O.B. Tysnes, J.P. Larsen, and G. Alves, *Risk and course of motor complications in a population-based incident Parkinson's disease cohort.* Parkinsonism Relat Disord, 2016. **22**: p. 48-53.
73. Poewe, W., A. Antonini, J.C.M. Zijlmans, P.R. Burkhard, and F. Vingerhoets, *Levodopa in the treatment of Parkinson's disease: an old drug still going strong.* Clinical Interventions in Aging, 2010. **5**: p. 229-238.
74. Hickey, P. and M. Stacy, *Deep Brain Stimulation: A Paradigm Shifting Approach to Treat Parkinson's Disease.* Front Neurosci, 2016. **10**: p. 173.
75. Doshi, P.K., N. Chhaya, and M.H. Bhatt, *Depression leading to attempted suicide after bilateral subthalamic nucleus stimulation for Parkinson's disease.* Mov Disord, 2002. **17**(5): p. 1084-5.
76. Okun, M.S., J. Green, R. Saben, R. Gross, K.D. Foote, and J.L. Vitek, *Mood changes with deep brain stimulation of STN and GPi: results of a pilot study.* J Neurol Neurosurg Psychiatry, 2003. **74**(11): p. 1584-6.
77. Hyam, J.A., M.L. Kringelbach, P.A. Silburn, T.Z. Aziz, and A.L. Green, *The autonomic effects of deep brain stimulation--a therapeutic opportunity.* Nat Rev Neurol, 2012. **8**(7): p. 391-400.
78. Ineichen, C., N.R. Shepherd, and O. Surucu, *Understanding the Effects and Adverse Reactions of Deep Brain Stimulation: Is It Time for a Paradigm Shift Toward a Focus on Heterogenous Biophysical Tissue Properties Instead of Electrode Design Only?* Front Hum Neurosci, 2018. **12**: p. 468.
79. Cagnan, H., T. Denison, C. McIntyre, and P. Brown, *Publisher Correction: Emerging technologies for improved deep brain stimulation.* Nat Biotechnol, 2019. **37**(10): p. 1237.
80. Gilletti, A. and J. Muthuswamy, *Brain micromotion around implants in the rodent somatosensory cortex.* J Neural Eng, 2006. **3**(3): p. 189-95.
81. Arcot Desai, S., C.A. Gutekunst, S.M. Potter, and R.E. Gross, *Deep brain stimulation macroelectrodes compared to multiple microelectrodes in rat hippocampus.* Front Neuroeng, 2014. **7**: p. 16.
82. Vedam-Mai, V., N. Krock, M. Ullman, K.D. Foote, W. Shain, K. Smith, A.T. Yachnis, D. Steindler, B.A. Reynolds, S. Merritt, F. Pagan, J. Marjama-Lyon, P. Hogarth, A.S. Resnick, P. Zeilman, and M.S. Okun, *The national DBS brain tissue network pilot study: A need for more tissue and for more standardization.* Movement Disorders, 2010. **25**(7): p. S456-S457.
83. Cenci, M.A. and M. Lundblad, *Ratings of L-DOPA-induced dyskinesia in the unilateral 6-OHDA lesion model of Parkinson's disease in rats and mice.* Curr Protoc Neurosci, 2007. **Chapter 9**: p. Unit 9 25.

84. Pouzat, C., O. Mazor, and G. Laurent, *Using noise signature to optimize spike-sorting and to assess neuronal classification quality.* Journal of Neuroscience Methods, 2002. **122**(1): p. 43-57.
85. Casanova, F., P.R. Carney, and M. Sarntinoranont, *Effect of needle insertion speed on tissue injury, stress, and backflow distribution for convection-enhanced delivery in the rat brain.* PLoS One, 2014. **9**(4): p. e94919.
86. Kozai, T.D.Y. and D.R. Kipke, *Insertion shuttle with carboxyl terminated self-assembled monolayer coatings for implanting flexible polymer neural probes in the brain.* Journal of neuroscience methods, 2009. **184**(2): p. 199-205.
87. Tseng, W.T., C.T. Yen, and M.L. Tsai, *A bundled microwire array for long-term chronic single-unit recording in deep brain regions of behaving rats.* J Neurosci Methods, 2011. **201**(2): p. 368-76.
88. Kil, D., M. Bovet Carmona, F. Ceyssens, M. Deprez, L. Brancato, B. Nuttin, D. Balschun, and R. Puers, *Dextran as a Resorbable Coating Material for Flexible Neural Probes.* Micromachines, 2019. **10**(1).
89. Lee, H.C., J. Gaire, S.W. Currlin, M.D. McDermott, K. Park, and K.J. Otto, *Foreign Body Response to Intracortical Microelectrodes Is Not Altered with Dip-Coating of Polyethylene Glycol (PEG).* Front Neurosci, 2017. **11**: p. 513.
90. Paralikar, K.J., J.K. Lawrence, and R.S. Clement, *Collagenase-aided insertion of intracortical microelectrode arrays: evaluation of insertion force and chronic recording performance.* Conference proceedings : Annual International Conference of the IEEE Engineering in Medicine and Biology Society IEEE Engineering in Medicine and Biology Society Annual Conference, 2006. **2006**: p. 2958-61.
91. Woeppel, K., Q. Yang, and X.T. Cui, *Recent Advances in Neural Electrode-Tissue Interfaces.* Curr Opin Biomed Eng, 2017. **4**: p. 21-31.
92. Thelin, J., H. Jorntell, E. Psouni, M. Garwicz, J. Schouenborg, N. Danielsen, and C.E. Linsmeier, *Implant Size and Fixation Mode Strongly Influence Tissue Reactions in the CNS.* Plos One, 2011. **6**(1).
93. Sohal, H.S., G.J. Clowry, A. Jackson, A. O'Neill, and S.N. Baker, *Mechanical Flexibility Reduces the Foreign Body Response to Long-Term Implanted Microelectrodes in Rabbit Cortex.* PLoS One, 2016. **11**(10).
94. Hess, A.E., J.R. Capadona, K. Shanmuganathan, L. Hsu, S.J. Rowan, C. Weder, D.J. Tyler, and C.A. Zorman, *Development of a stimuli-responsive polymer nanocomposite toward biologically optimized, MEMS-based neural probes.* Journal of Micromechanics and Microengineering, 2011. **21**(5).
95. Lai, H.Y., L.D. Liao, C.T. Lin, J.H. Hsu, X. He, Y.Y. Chen, J.Y. Chang, H.F. Chen, S. Tsang, and Y.Y.I. Shih, *Design, simulation and experimental validation of a novel flexible neural probe for deep brain stimulation and multichannel recording.* Journal of Neural Engineering, 2012. **9**(3).
96. Weltman, A., J. Yoo, and E. Meng, *Flexible, Penetrating Brain Probes Enabled by Advances in Polymer Microfabrication.* Micromachines, 2016. **7**(10).

97. Butson, C.R., C.B. Maks, and C.C. McIntyre, *Sources and effects of electrode impedance during deep brain stimulation.* Clinical Neurophysiology, 2006. **117**(2): p. 447-454.
98. Prasad, A. and J.C. Sanchez, *Quantifying long-term microelectrode array functionality using chronic in vivo impedance testing.* Journal of Neural Engineering, 2012. **9**(2).
99. Ward, M.P., P. Rajdev, C. Ellison, and P.P. Irazoqui, *Toward a comparison of microelectrodes for acute and chronic recordings.* Brain Research, 2009. **1282**: p. 183-200.
100. Golabchi, A., B.C. Wu, X. Li, D.L. Carlisle, T.D.Y. Kozai, R.M. Friedlander, and X.T. Cui, *Melatonin improves quality and longevity of chronic neural recording.* Biomaterials, 2018. **180**: p. 225-239.
101. Rennaker, R.L., J. Miller, H. Tang, and D.A. Wilson, *Minocycline increases quality and longevity of chronic neural recordings.* Journal of Neural Engineering, 2007. **4**(2): p. L1-L5.
102. Vedam-Mai, V., N. Krock, M. Ullman, K.D. Foote, W. Shain, K. Smith, A.T. Yachnis, D. Steindler, B. Reynolds, S. Merritt, F. Pagan, J. Marjama-Lyons, P. Hogarth, A.S. Resnick, P. Zeilman, and M.S. Okun, *The national DBS brain tissue network pilot study: need for more tissue and more standardization.* Cell and Tissue Banking, 2011. **12**(3): p. 219-231.
103. Chiken, S. and A. Nambu, *Mechanism of Deep Brain Stimulation: Inhibition, Excitation, or Disruption?* Neuroscientist, 2016. **22**(3): p. 313-22.
104. Eisenstein, S.A., W.B. Dewispelaere, M.C. Campbell, H.M. Lugar, J.S. Perlmutter, K.J. Black, and T. Hershey, *Acute Changes in Mood Induced by Subthalamic Deep Brain Stimulation in Parkinson Disease Are Modulated by Psychiatric Diagnosis.* Brain Stimulation, 2014. **7**(5): p. 701-708.
105. Wertheimer, J., A.Y. Gottuso, M. Nuno, C. Walton, A. Duboille, M. Tuchman, and L. Ramig, *The impact of STN deep brain stimulation on speech in individuals with Parkinson's disease: The patient's perspective.* Parkinsonism & Related Disorders, 2014. **20**(10): p. 1065-1070.
106. Schupbach, W.M.M., S. Chabardes, C. Matthies, C. Pollo, F. Steigerwald, L. Timmermann, V.V. Vandewalle, J. Volkmann, and P.R. Schuurman, *Directional Leads for Deep Brain Stimulation: Opportunities and Challenges.* Movement Disorders, 2017. **32**(10): p. 1371-1375.
107. Reker, P., T.A. Dembek, J. Becker, V. Visser-Vandewalle, and L. Timmermann, *Directional deep brain stimulation: A case of avoiding dysarthria with bipolar directional current steering.* Parkinsonism & Related Disorders, 2016. **31**: p. 156-158.
108. Mccreery, D.B., W.F. Agnew, T.G.H. Yuen, and L. Bullara, *Charge-Density and Charge Per Phase as Cofactors in Neural Injury Induced by Electrical-Stimulation.* Ieee Transactions on Biomedical Engineering, 1990. **37**(10): p. 996-1001.
109. Kuncel, A.M. and W.M. Grill, *Selection of stimulus parameters for deep brain stimulation.* Clinical Neurophysiology, 2004. **115**(11): p. 2431-2441.

110. Lundgren, S., T. Saeys, F. Karlsson, K. Olofsson, P. Blomstedt, J. Linder, E. Nordh, H. Zafar, and J. van Doorn, *Deep Brain Stimulation of Caudal Zona Incerta and Subthalamic Nucleus in Patients with Parkinson's Disease: Effects on Voice Intensity.* Parkinsons Disease, 2011. **2011**.
111. Burrows, A.M., P.D. Ravin, P. Novak, M.L.B. Peters, B. Dessureau, J. Swearer, and J.G. Pilitsis, *Limbic and Motor Function Comparison of Deep Brain Stimulation of the Zona Incerta and Subthalamic Nucleus.* Neurosurgery, 2012. **70**.
112. Blomstedt, P., R.S. Persson, G.M. Hariz, J. Linder, A. Fredricks, B. Haggstrom, J. Philipsson, L. Forsgren, and M. Hariz, *Deep brain stimulation in the caudal zona incerta versus best medical treatment in patients with Parkinson's disease: a randomised blinded evaluation.* Journal of Neurology Neurosurgery and Psychiatry, 2018. **89**(7): p. 710-716.
113. Bouthour, W., P. Megevand, J. Donoghue, C. Luscher, N. Birbaumer, and P. Krack, *Biomarkers for closed-loop deep brain stimulation in Parkinson disease and beyond (vol 15, pg 343, 2019).* Nature Reviews Neurology, 2019. **15**(6): p. 363-363.